Tribological Study of Al-RHA MMC under Lubricated Condition

Thesis submitted in partial fulfillment

of the requirement for the degree of

Master of Engineering

By

Morsalim Mollick

Examination Roll number: **M4MEC23001**

Registration number: **136473** of **2016-2017**

Under the guidance of

Dr. Shouvik Ghosh

DEPARTMENT OF MECHANICAL ENGINEERING

FACULTY OF ENGINEERING &TECHNOLOGY

JADAVPUR UNIVERSITY

KOLKATA, INDIA

2023

FACULTY OF ENGINEERING AND TECHNOLOGY
JADAVPUR UNIVERSIT

CERTIFICATE OF APPROVAL *

This foregoing thesis is hereby approved as a credible study of an engineering subject carried out and presented in a manner satisfactory to warrant its acceptance as a prerequisite to the degree for which it has been submitted. It is understood that by this approval the undersigned do not endorse or approve any statement made, opinion expressed or conclusion drawn therein but approve the thesis only for the purpose for which it has been submitted

*Only in case the thesis is approved

FACULTY OF ENGINEERING AND TECHNOLOGY
JADAVPUR UNIVERSITY

We hereby recommend that the thesis presented under our supervision by ***Mr Morsalim Mollick*** *entitled "****Tribological Study of Al-RHA MMC under Lubricated Condition****" be accepted in partial fulfillment of the requirements for the degree of Master of Mechanical Engineering.*

Thesis Advisor _____

Dean of Faculty of Engineering
and Technology

Acknowledgments

I would like to express my heartfelt gratitude to all the individuals and organizations who have supported me during the research and writing of this thesis. Their contributions have been invaluable, and without their help, this work would not have been possible.

First and foremost, I extend my deepest appreciation to my supervisor, **Dr Shouvik Ghosh**, for their unwavering guidance and insightful feedback throughout this research endeavour. Their expertise and encouragement have been instrumental in shaping the direction of this thesis.

I am indebted to the faculty members of the Mechanical Engineering for their academic rigor, and fostering an environment of intellectual growth. Their commitment to education has been a constant source of inspiration.

I would like to thank the staff and administrators of **Jadavpur University** for their administrative support and for providing access to the necessary resources for conducting research. Their efficiency and assistance have been of great help.

I am grateful to my friends and classmates who have been a constant source of motivation, encouragement, and a listening ear during moments of doubt. Your support has been crucial in sustaining me through the challenges of this academic pursuit.

My deepest appreciation goes to my family for their unconditional love and support throughout my academic journey. Their belief in me and encouragement during moments of self-doubt have been my driving force.

Finally, I would like to express my gratitude to all the researchers and scholars whose works have paved the way for this thesis. Their contributions to the field have been invaluable and have inspired me to explore new avenues of knowledge.

In conclusion, I acknowledge and appreciate the collaborative efforts of all those mentioned above, as well as anyone else whose contributions might have been inadvertently omitted. Each one of you has played an essential role in shaping this thesis, and I am sincerely thankful for your support.

Date:

_____

(Morsalim Mollick)

ABSTRACT

Metal matrix composites (MMCs) are materials that incorporate reinforcement materials to enhance their properties. One significant challenge associated with MMCs is the elevated cost of the reinforcement materials. To overcome this obstacle, it becomes necessary to explore affordable alternatives such as Rice Husk Ash (RHA). The present research investigates the Mechanical and Tribological Properties, specifically hardness and wear of aluminium alloy Al6061 reinforced with RHA using the stir casting technique. The volume fraction of RHA reinforcement varies between 4% and 12% by volume fraction. The tribological results are optimized using Taguchi method and Grey relational analysis. Micro-hardness tests were conducted on a Vickers micro-hardness tester reveal that the alloy's micro-hardness increases as the volume fraction of the reinforcement rises. Moreover, the wear decreases with higher volume fractions of RHA, indicating improved wear resistance for the composite material. In summary, the addition of RHA reinforcement enhances the mechanical and tribological properties of the aluminium alloy Al6061, as supported by the conducted studies.

Keywords: Rice Husk Ash, Aluminium, Hardness, Wear.

Chapter 1

Introduction

1.1 Introduction

Tribology is the scientific study of rubbing or sliding of materials against one another on moving surfaces. It encompasses studies on lubrication, wear, and friction, among other topics. The word "tribology" comes from the Greek words " tribos " which means "rubbing," and "logos," which means "study." Therefore, the study of rubbing surfaces is what the name "tribology" refers to. Tribology is a branch of research that draws from a variety of disciplines, including physics, chemistry, engineering, and material science. Tribology is an interdisciplinary field. It's possible that a material with good tribological properties won't have any good mechanical qualities, and the opposite is also possible. It is unusual for a material to possess both good mechanical and tribological characteristics. We need a material that possesses tribological and mechanical properties that are adequate for the Metal Matrix Composite for a variety of applications. This material must be available to us.

A composite material is a substance that is produced by combining two or more components to form a substance that possesses features that are not shared by the individual components that were used to create it. Even after being combined, the individual components of a composite do not lose their own identities. A composite material is made up of a continuous phase matrix as well as one or more discontinuous phases, which are frequently referred to as reinforcement.

Metal matrix composite is used extensively these days in a variety of industries including automotive, aerospace, and electronics.

We are able to tailor the density, mechanical capabilities, tribological features, and corrosive qualities of an MMC by modifying the types, sizes, and amounts of reinforcement.

1.2 Aluminium Matrix Composites

Intensifying demands for increased life service and weight reduction, and hence lower product prices, drive the research and implementation of new materials. The rising use of

composite materials is mostly due to their superior physical-mechanical and tribological capabilities over matrix materials.

Aluminium and its alloys are commonly used as composite matrix materials due to its favourable properties such as low density, strong thermal conductivity, and corrosion resistance, low production cost, and high recycling potential. Aluminium alloy-based composite materials are increasingly being employed in the aviation, aerospace, automotive, and military industries. They are used in the manufacture of engine blocks, cylinder liners, connecting rods, crankshafts, camshafts, cardan shafts, helicopter propellers, and brake discs and drums for vehicles and railways.

The mechanical and tribological properties of aluminium composites are improved by the addition of appropriate reinforcements and improvers, carbides, borides, nitrates, and oxides, such as Al_2O_3, SiC, TiC, TiO_2, B_4C, TiB_2, WC, and others, are commonly used reinforcements. The size and amount of reinforcement used are determined by the manufacturing process as well as the actual application of the composite material.

A hybrid composite is created by combining two or more reinforcements with the matrix material. However, in recent years, there has been a tendency toward the use of nano-scale reinforcements and the production of nano-composites.

1.3 Types of Reinforcements

There are several types of reinforcing materials utilised in fabrication of MMCs. When it comes to defining the overall performance of a composite material, the reinforcement plays a very important role. The mechanical, thermal, and electrical properties of the composite can be greatly impacted by the size, shape, distribution, and volume percent of the reinforcement.

1.3.1 Ceramic Particulate

Ceramic reinforcements can be manufactured as continuous fibre, short fibre, whisker, or particle. Continuous ceramic fibres have a lot of potential for strengthening composite materials. They are appealing as reinforcements in high temperature structural materials because they combine relatively high strength and elastic modulus with high temperature capacity and general resistance to environmental damage. Some significant ceramic reinforcements tabulated in above Table 1.1.

Table 1.1-Different Types of reinforcement

Particle	SiC, TiC, Al_2O_3
Whiskers	SiC, TiB_2, Al_2O_3
Short fibers	Glass, Al_2O_3, SiC, (Al_2O_3+SiO_2,)
Oxide	Al_2O_3, (Al_2O_3+ SiO_2), ZrO_2, silica-based glasses
Non-oxide	B_4C, SiC, Si_3N_4, BN

1.3.2 Industrial Waste

Industrial waste has the potential to provide alternative reinforcing materials that are cheap, easy to obtain, and have physical and mechanical qualities comparable to conventional particles. Industrial waste reinforcement examples include fly ash and red mud. The waste material generated during the alumina production in aluminium industry is known as red mud. Red mud waste increased due to the increased aluminium production during the past few years. 1.5 tonnes of red mud are generated for every 2.5 tonnes of alumina produced. The aluminium industry provides about 120 million tonnes of red mud annually. More than 100 million tonnes of ash (fly ash, bottom ash, and slag) are created by the burning of coal in the United States. These solid particles come from non-combustion components of the coal.

1.3.3 Agro Waste

Agricultural wastes high in oxide material can be used as an alternative material in metal matrix composites. RHA (Rice Husk Ash) is a type of agricultural waste that is found all over the world. RHA is derived from the rice milling process, which yields rice, bran, and husk, all of which are used as fuel in the rice milling process. The burning residue is known as RHA

The Al-MMCs are fabricated by various processes like powder metallurgy (PM), stir casting, squeeze casting, friction stir processing, etc. Different types of Al-Alloys are used as matrixes are Al6061, LM6, A356, Al7075, Al7009, Al2024 etc. Commonly used reinforcement for Al-MMCs are Al_2O_3, SiC, TiC, TiO_2, B_4C, TiB_2, WC etc. In this review it is discussed about changing in various mechanical properties and tribological properties of Al-MMC by varying volume % or mass % of reinforcements.

1.4 Mechanical behavior of Al MMC

Over the course of the last several decades, a significant number of researchers have contributed to the subject of metal matrix composites by conducting research on the mechanical properties of a variety of metal matrix composites.

Devanathan et al. [1] observed the addition of SiC, CSA, and FA particles increases the hardness of matrix alloy AA6061. As the reinforcement particles rises, the Brinell hardness and tensile strength of MMHCs increases linearly. The presence of reinforcement in the matrix, which reduces matrix particle size and increases reinforcement surface area. SiC, CSA, and FA particles take up more surface area in the matrix, which provides strong resistance to plastic deformation and lowers ductility, increasing the hardness of MMHCs.

Rao et al. [2] observed improved mechanical properties during compression when a greater quantity of fly ash was included in the MMCs. The density of the composites decreased while their hardness increased as compared to the basic alloy when the quantity of fly ash added was increased up to 10 vol. percent.

Mindivan et al. [3] found adding fly ash particles to AA6061/Al using solid state process and two-phase matrixes results in an increase in hardness, compressive strength, and wear resistance while simultaneously resulting in a decrease in density and electrical conductivity.

Verma et al. [4] noticed in their experiment the hardness of an Al6063/Fly Ash composite increased as the amount of fly ash increased up to 9 volume %, while at the same time, the fatigue strength declined. And using S/N ratio it was observed that fly ash volume % is the most significant factor for wear.

Bharathi et al [5] found that the increase in fly ash % upto 5 % in stir cast Aluminium-FA composite led to an increase in the material's hardness. Fly ash particle also caused increase in stiffness and strength of the composite material.

Dinharan et al. [6] observed that incorporation of FA particles resulted in an increase in the micro-hardness of the composite. The results of the micro-hardness tests indicated values ranging from 62 HV at 0 volume percent to 125 HV at 18 volume percent.

Reddy and Srinivas [7] found that increasing the amount of fly ash and SiC content in the Al MMC led to an increase in the ultimate tensile strength as well as its hardness up to 7.5 volume %.

Kumar et al [8] concluded that there is a clear connection between the proportion of fly ash in a material's weight and its wear, tensile strength, impact strength, and hardness. The inabilities of the aluminium alloy to deform as a result of the addition of fly ash contribute to an improvement in the material's hardness, tensile strength, and wear resistance. The density of the composites decreased as the % by weight of fly ash particles in the mixture increased. Hardness, tensile strength, and wear resistance all demonstrated a connection with particle size that was inversely proportionate. Greater hardness and tensile strength could be achieved with particles of larger size.

Sanmugsundaram et al. [9] examined hardness, tensile strength, and compressive strength was respectively, for the test materials. When there was a higher % of fly ash in the aluminium, the material had a higher tensile strength. The decrease in solid solution strengthening and particle clustering, on the other hand, causes the tensile strength to begin to lessen after the quantity of fly ash reaches 15 weight percent. It was discovered that increasing the quantity of fly ash in composites increased their hardness as well as their compressive strength. When composites contain more than 20 weight % of fly ash, their hardness and compressive strength begin to decrease.

Selvam et al [10] found out the incorporation of fly ash particles into AMCs resulted in an increase in both the micro-hardness and the tensile strength of the materials. When compared to an unreinforced AA6061 alloy, the AA6061/12 wt. % fly ash AMC displayed micro-hardness that were 132.21 % greater and had a UTS that was 56.95 % higher.

Suragimath and Purohit [11] found out tensile strength begins to increase when the weight % of Fly Ash increases, the increase in the weight % of fly ash results in an increase in the impact strength of hybrid composite materials.

1.5 Tribological behavior of Al-MMC

Mindivan et al [3] recycled using the solid-state technique, AA6061/Al alloy chips of varying sizes as well as fly ash particles and looked at the effect that chip size and fly ash content had on the microstructure, as well as the mechanical and wear parameters of recycled AA6061/Al two-phase composites. The microstructural evaluation showed a satisfactory interface between the fly ash particulates and the AA6061/Al two phase matrixes. Additionally, the fly ash particles were distributed in an even manner throughout the recycled composites that contained fine chips. The integration of fly ash particles into the AA6061/Al two-phase matrix provided a reasonable increase in hardness, compressive strength, and wear resistance, as indicated by the findings obtained from mechanical testing and wear testing. In comparison to the action of the Al_2O_3 ball, the destructive potential of the steel ball was significantly less when applied to the recycled composites fine chips.

Natarajan et al. [12] observed increasing the amount of fly ash in the brake pad causes both the weight of the brake liner and the coefficient of friction to drop. This makes the brake pad suitable for use in light automobiles.

Santhosh et al. [13] found out that wear was shown to be reduced by approximately 1.6 times as the amount of fly ash increased. Ceramic particles in the form of silicates, carbides, and oxides have been detected in the wear debris using SEM, XRD, and EDS. These ceramic particles serve to minimise the wear that is caused by dry sliding on aluminium composites.

Bharathi et al. [5] observed the abrasive wear resistance of MMC has improved with an increase in fly ash content as a result of the increased hardness, stiffness, and strength of the reinforced fly ash particle. However, the rate of wear has increased with an increase in load and speed. This is due to the fact that linkages between the reinforcing particle and the matrix material have broken, as well as the fact that friction has increased at the contact surfaces, the three most common forms of wear mechanisms are scratching, delamination, and ploughing.

Dinharan et al. [6] found out the resistance of the composite to wear was significantly improved by the addition of FA particles. The rate of wear slowed down in response to the growing volume fraction of FA particles. It was found that the wear rate was $411 \text{ x } 10^{-5} \text{ mm}^3/\text{m}$ when there was 0% volume, but it dropped to $203 \text{ x } 10^{-5} \text{ mm}^3/\text{m}$ when there was 18 % volume. The particles had an effect on the manner in which wear occurred as well as the shape of the debris produced by wear. Because of an increase in the volume% of FA particles, the mode of wear shifted from adhesion to abrasion as a result of this modification, the wear debris assumed the shape of thin plates when the volume fraction was 0 %, but it became spherical when the volume fraction was 18 %.

Sharma et al. [14] found out the fly ash content of the manufactured composites should be increased so that they have a higher resistance to wear, composites with higher levels of fly ash content saw 13.6 % less wear than those with lower levels of fly ash concentration.

Kumar et al. [8] noticed the rate of wear caused by dry sliding was shown to be inversely proportional to particle size. The amount of fly ash contributed to a decrease in the rate of wear, the applied load has a direct influence on the wear rate as well, with the wear rate increasing with larger loads and vice versa.

P.R.S. Kumar et al. [15] found out AA6061-fly ash composites in the T6 heat treated state exhibited superior wear behaviour when compared to the matrix alloy at both low and high temperatures. This is because to the even distribution of solid fly ash particles throughout the composite. An important result of this research is that composites can withstand temperatures of up to 300 degrees Celsius while exhibiting resistance to transition wear ranging from mild to severe.

This is because of the action that fly ash particles have subsurface hardening property on the surface. Instead, the matrix phase of the AA6061 alloy has undergone severe plastic deformation, which has caused the matrix alloy to exhibit mild-to-severe transition wear above 200 degrees Celsius.

Razzaq et al. [16] found out, the addition of FA particles to AA6063 alloy has a considerable effect on the way the material behaves when subjected to wear. The wear rate is reduced in proportion to the increase in the weight content of FA reinforcements. The results of this experiment imply that raising the FA concentration while keeping the sliding speed

constant will result in increased wear resistance. In addition to this, the rate of wear increases with an increase in the load that is being applied.

Rohatgy et al [17] observed the abrasion wear resistance of the alloy having 5 vol.% fly-ash was found to be superior to that of the base A356 alloy under a load of 8 N and at sliding velocities of 1 and 2 m/s. This abrasion wear resistance was found to be comparable to that of aluminium alloys containing alumina fibres. It is possible that the SWR (specific wear rate) of the composite increased beyond that of the base alloy once this load was applied, and that this was caused by the de-bonding and fracturing of fly ash particles. The accumulation of worn debris in the spaces between the abrasive particles, which ultimately leads to a drop in the depth of penetration and a change from two-body to three-body wear, has been postulated as the explanation of the observed decrease in SWR with a rise in load. This effect can also be seen in the higher SWR that was obtained when travelling at 1 m/s rather than 2 m/s. The rapid increase in SWR that occurs as the abrading particle size increases between 20 and 30 mm has been connected to the significant contribution made by micro cutting in this range of abrading particle size. The composite, on the other hand, has a smaller magnitude of increase, and this can be attributed to the larger contribution of delamination wear. It has been determined that the composite has a coefficient of friction during abrasion that falls somewhere in the range of 0.45 and 0.75, depending on the testing conditions. In contrast, the changing trend of the coefficient of friction with load or abrading particle size is not the same as what was observed in tests in which sliding was not repeated on the same track. The observed trend of decreasing friction with an increase in load or abrading particle size is also attributable to the accumulation of wear debris, which results in an adjustment in the mechanism of wear. This is one of the primary causes of the phenomenon. Abrasion of the composite is seen to occur in addition to micro-cutting caused by delamination. This is caused by cracks propagating from the rubbing surface to the subsurface through the fly ash-matrix interface and the interfaces of silicon particles, which are more prevalent in a composite possibly as a result of a chemical reaction between fly ash particles and the molten base alloy during processing. Micro-cutting is also seen to occur as a result of abrasion of the composite. During the tests that were carried out as part of this investigation, three different bodies were subjected to wear, as demonstrated by the wear coefficients for both the base alloy and the composite.

Wear characteristics of the test materials were observed by Sanmugsundaram et al [9]. Fly ash particles were added to commercial aluminium in order to greatly enhance its wear resistance. Composite materials beat unreinforced aluminium throughout the entire load range assessed under dry sliding conditions. Fly ash particles were applied to commercial aluminium in order to significantly increase its wear resistance.

It was possible that this is because of the positive impact that fly ash particles have, as these particles dominate the components that affect wear resistance. However, lowering the wear loss of the aluminium by only twenty percent using fly ash particles was a very successful endeavour.

Senthilkumar et al [18] found out an increase in the amount of reinforcement, such as boron carbide and fly ash, results in an increase in the friction coefficient. The performance of this hybrid composite shoe degraded under greater loads, and the load's value increased in proportion to the increase in the shoe's coefficient of friction. The amount of wear loss experienced by the composite specimen is proportional to the % of reinforcement present. Examples of reinforcement include boron carbide and fly ash. When the proportion of reinforcement is increased to a higher value by employing fly ash and boron carbide as reinforcement, the value of hardness will decrease. This is because the proportion of reinforcement is lower. When compared to the hardness of the aluminium alloy, which is approximately 55 BHN, the hardness value of the aluminium alloy LM6 reinforced with 3 % of boron carbide and fly ash is greater than the hardness value of the aluminium alloy LM6. This is due to the fact that the hardness value increases when the volume % of reinforcement increases after 3 %, such as when it increases from 6 % to 9 %.

Shaikh and Shaikh [19] found that When contrasted with unreinforced Al–SiC composites and the base matrix composed of Al, 10 % SiC and 10 % fly ash had better hardness and wear resistance.

Balasubramaniam et al. [20] noted both unreinforced Al7075 and a larger concentration of reinforcements can minimise wear by up to 62% in conditions characterised by low load and low sliding velocity. When subjected to high loads and low sliding velocities, the wear rate can be cut by as much as 49 % when using hybrid composites. At low load and medium sliding velocity, as well as high load and medium sliding velocity, the wear rate is reduced by up to 54 % when compared to pure Al7075 composites. This holds

true for both situations. At low load and high sliding velocity, the wear rate is reduced by up to 38 % in comparison to a pure Al7075 alloy. Under maximum load and at high sliding velocity, the wear rate can be reduced by up to 16% in hybrid composites. The value of the wear rate goes up when the load that is placed on the composites goes up, but it goes down as the weight % of B4C and CSFA particles that are included within Al7075 composites goes up. The Adhesive wear mechanism of Al7075 alloy was observed here. It has been observed that hybrid composites were subjected to abrasive wear.

Sudarshan and Surappa [21] noticed, adding fly ash particles to A356 Al alloy at a volume fraction of 6 volume percent can reduce dry sliding wear rates at low loads (10 and 20 N). When it comes to wear, unreinforced alloys are more likely to experience adhesive wear while composites are more vulnerable to abrasive wear. Subsurface delamination is the primary mechanism that leads to failure in both alloys and composites when they are subjected to higher loads.

Virkunwar et al. [22] noticed during tribological test that the composite goes through both adhesive and abrasive wear mechanisms, with the latter being the more common of the two. The wear behaviour of metal matrix composites based on aluminium and reinforced with rice husk ash was observed in a dry sliding test employing a pin-on-disc configuration against hardened tool steel. The test was carried out in a dry environment. The loads were restricted to a range of 10 to 30 N, while the sliding speeds were confined to a range of 0.2 to 5.0 metres per second.

1.6 Mechanical behavior of Al-RHA

In the past few decades, a great number of researchers have investigated the possibility that agro waste such as rice husk ash can be utilised as a reinforcing material for the purpose of increasing the mechanical properties of AMCs.

Olusesi, O.S. et. al. [24] noticed the AA6061/clay + RHA composite was successfully manufactured by utilising the stir casting method with a variety of different weight percent of reinforcement, including 2.5, 5, 7.5, and 10 %. In comparison to the mechanical properties of AA6061 aluminium alloy, the composite exhibited significant improvements. When compared to the other composite weight reinforcements, the 7.5 weight percent reinforcement exhibited superior hardness qualities.

Prasad and Kumar [25] found, the degree of hardness of the material grows in proportion to the amount of rice husk ash that is present in A356.2/RHA composites.

Gupta et al. [26] noted the micro-hardness of the composite that contained 5 weight percent of RHA was found to be 15.08 percent higher than the micro-hardness of the unreinforced AA7075, whereas the micro-hardness of the composite that contained 5 weight percent of CES was found to be 4.519 percent lower than the micro-hardness of the unreinforced AA7075.

1.7 Tribological behavior of Al-RHA composite

Al-RHA MMCs have attracted a great deal of interest during the past few decades. The researchers looked at how various testing variables, such as weight, sliding speed, sliding distance, and volume fraction of reinforcement, affected the material's tribological behaviour.

Gladston et al. [27] noticed RHA particles contributed to an increase in the composites' resistance to wear. They were able to reduce the size of the wear debris that was created as well as the plastic distortion of the surface that was worn. There were a number of elements that contributed to an increase in wear resistance, including increased hardness, the generation of strain fields, homogeneous distribution, the spherical shape of RHA particles, and a reduction in the effective contact area. The wear mode transformed from adhesive to abrasive as the volume percent of RHA in the material increased. The tension that was applied to the composite caused an acceleration in its rate of wear. A greater amount of material is removed as a direct consequence of the increased penetration of counter-face asperities and the subsequent softening of the pin surface. The increase in load sped up the process of pit development and plastic deformation, both of which were undesirable outcomes, the size of the worn debris increased along with the load.

Kumar and Kumar [28] observed when subjected to tribological testing conditions, the AA7075-B4C-RHA hybrid composite demonstrates a decrease in wear rate in proportion to an increase in normal load, under conditions of steady state, the specific wear rate of hybrid composites increases as the sliding velocity also increases.

Prasad and Kumar [25] made the observation that the rate of wear decreases as the weight percentage of RHA particles in the material increases. As the wt. percent of RHA particles in the alloy A356, increases, the friction coefficient of the material decreases. When

there is a greater proportion of reinforcing by weight, the size of the wear debris produced is proportionally smaller.

Gupta et al. [26] noted Samples containing 5 wt. % RHA were found to have the lowest wear loss across all test loads and sliding speeds; on the other hand, composites containing 3.75 wt. % and 5 wt. % CES (carbonized eggshells) showed the most wear loss at higher loads, wear resistance was raised by 50 % and 10.80 % at 10N and 50 N, respectively. It was revealed that the rate of wear loss increased with both the weight applied and the sliding speed. This was the case regardless of the composition. The sample with 3.75 weight percent RHA and 1.25 % CES had the highest COF when evaluated under a range of sliding conditions. This increase in the COF of the fundamental composition was 5 % at 10N and 13.2 % at 50N, respectively, when compared to the initial composition. The coefficient of friction (COF) increased with increasing weight across all composite samples but decreased with increasing sliding speed. The key wear mechanisms are severe delamination and ploughing markings when 30N is applied at a slow speed of 1 m/s. On the other hand, when 30N is applied at a fast speed of 5 m/s, the primary wear mechanisms are mild delamination and increased ploughing.

Vinod et. al. [29] noticed using a pin-on-disk device. Analysing the dry sliding wear behaviour of A356 (Al-7Si-0.35Mg)/RHA/FA Composite against EN 31 stainless steel discs of 100 mm diameters and 8 mm thickness under a variety of applied loads, sliding speeds, and sliding distances, when compared to the matrix composed of alloy, the author asserts that the incorporation of RHA and fly ash into the A365 matrix increases wear resistance while simultaneously reducing the amount of wear debris. When compared to the as-cast alloy, the wear resistance capabilities of the hybrid composite material A356/7.5 percent RHA-7.5 percent fly ash are superior.

1.8 Lubrications for reducing wear

Lubrication is the process of minimizing wear and friction caused dynamic contact surface the application of a coating. Lubricating a surface can be accomplished with a wide variety of different substances. The most common types of lubricants are oil and grease; however, a wide variety of other types of lubricants are also used to reduce the amount of friction and wear that occurs between two moving surfaces that are in touch.

Around 2400 BC, water, bitumen, and oils extracted from plants and animals were utilised as lubricants by local inhabitants. A lubricant is a substance, which can either be organic or inorganic. Lubricants also used to reduce the amount of heat that is produced when the surfaces move.

1.9 Types of lubricant

Lubricants are compounds that are often used to reduce the amount of friction that occurs between parts that are in touch with one another. Lubricants, depending on the type, can also perform a variety of other activities, such as regulating heat, transmitting power, sealing against dust or dirt, decreasing oxidation, and preventing corrosion. Lubricants can also perform these services in addition to preventing corrosion and lowering oxidation. Lubricants are most frequently found in liquid or semi-solid form, although they can also be found in other configurations. Some example of solid lubricants are- Graphite, Molybdenum disulphide, Polytetrafluoroethylene. Grease is an example of semi-solid lubricants. Water, as well as natural or manufactured oils, fall under the category of liquids. Air is an example of a gas lubricant.

These lubricants have widespread application across a variety of business sectors, including the automotive, aerospace, construction, chemical, and textile industries, among others, to facilitate the efficient operation of the machinery and equipment utilised in those sectors.

1.10 Present work

The focus of the current research is on the investigation of the mechanical and tribological properties of metal matrix composites made of Al-RHA. Altering the tribological testing parameters allows for the optimisation of the various features of the composite. Hardness, wear, and friction are some of the properties that were investigated in this work in relation to composites made of Al-RHA. There is a range of options for the volume proportion of reinforcement, from 4 to 12 %. It was determined which composite samples had the hardest surface. In order to determine whether or not composites are suitable for use in multi-tribological applications, a study is carried out in which wear and friction are both taken into consideration as response variables.

1.11 Closure

The purpose of this chapter is to provide a literature overview of metal matrix composites, with a specific concentration on the Al-RHA metal matrix composite. On this subject, an exhaustive evaluation of the relevant published literature is provided, and discussion of the applicability of composites is also included. In addition, a synopsis of the present study is provided alongside the framework of the thesis.

Chapter 2

Basic Consideration

2.1 Introduction

A composite material is an amalgamation of two or more constituent materials, which differ significantly from one another chemically or physically, are combined to produce a material having characteristics that are distinct from those of the constituent materials. The finished composite material's individual components stay distinct and independent, setting composites apart from solid solutions. A composite material can be classified in two ways a) by the types of matrix material like polymeric matrix composites, metal matrix composites, ceramic matrix composites b) by the types of reinforcements like whisker reinforced composite, particle reinforced composites, fiber reinforced composites, laminated composites etc.

Metal matrix composites (MMC) are type of composites which consists of metal as a matrix. Metal Matrix composites got huge attention from engineers and scientist because different mechanical properties can be got by changing the size or changing the amount of reinforcement. Because of its low density, high wear resistance, high thermal resistance, high corrosion resistance and hardness Al-MMC's has huge demand in aerospace and automobile industries. Wear in machinery is the major cause of loss in Industries due to maintenance and replacement of equipment's. Losses due to wear can be reduced by tailoring suitable nano-composite using perfect type of reinforcement with optimum size and amount.

2.2 Fabrication Process of MMCs

Metal matrix composites (MMC) fabrication is classified into three types: solid, liquid, and gaseous state. Fabrication process also determines the mechanical and tribological properties of metal matrix composites.

2.2.1 Methods based on solid state

i. Powder blending and consolidation (powder metallurgy):

Powdered metal and discontinuous reinforcement are blended and bonded via compaction, degassing, and thermo-mechanical treatment (perhaps via hot isostatic pressing (HIP) or extrusion). The three basic processes of the powder metallurgy press and sinter process are powder blending (pulverisation), die compaction, and sintering. Compaction is typically done at room temperature, and sintering is often done at elevated temperatures while maintaining atmospheric pressure and carefully regulated atmosphere composition. To get unique features or higher precision, optional further processing like coining or heat treatment sometimes comes next. The process of mixing fine (180 microns) metal (typically iron) powders with additives like a lubricant wax, carbon, copper, and/or nickel, pressing them into a die of the desired shape, and then heating the compressed material ("green part") in a controlled atmosphere to bond the material by sintering is one of the more traditional of these techniques and is still used to produce about 1 metric ton/year of structural components of iron-based alloys. This results in precision pieces that are often extremely near to the die dimensions but have sub-wrought steel characteristics due to their 5–15 % porosity. Over the past fifty years, a number of other PM procedures have been created. These consist of:

i. (a). Powder forging:

A "preform" created by the traditional "press and sinter" technique is heated and then hot forged to full density, producing qualities that are nearly identical to those of the original metal.

i. (b). Hot isostatic pressing (HIP):

In this process, the powder, which is typically spherical and gas atomized, is poured into a mould made of a suitable-shaped metallic 'can'. The can is shaken before being emptied and shut. It is then put into a hot isostatic press, heated to a homologous temperature of about 0.7, and exposed for a number of hours to an external gas pressure of about 100 MPa (1000 bar, 15,000 psi). As a result, a fully dense, formed item with as-wrought or better characteristics is produced. HIP was

created in the 1950s and 1960s and began to be produced in tonnes in the 1970s and 1980s. 25,000 ton/year of stainless and tool steels, as well as significant components of super alloys for jet engines, were produced using it in 2015.

i. (c). Metal injection moulding (MIM):

In this process, the powder, which is typically very fine (less than 25 microns) and spherical, is combined with a plastic or wax binder to nearly the maximum solid loading, usually 65vol %, and then injection moulded to create a "green" part with intricate geometry. The binder is then removed from this component (debinding) using heat or another treatment, resulting in a "brown" section. After being sintered, this component shrinks by about 18 %, producing a finished part that is complicated and 95–99 % dense (surface roughness: 3 microns). Invented in the 1970s, production has grown steadily since 2000, with an estimated 12,000-ton global volume worth €1265 million in 2014.

i. (d) Electric current assisted sintering (ECAS):

Electric current assisted sintering (ECAS) technologies use electric currents to densify powders. They have the advantage of drastically cutting production time (from 15 minutes for the slowest ECAS to a few microseconds for the fastest), allowing close to theoretical densities, and not needing a long furnace heat. However, they have the disadvantage of producing only simple shapes. Due to the potential of direct sintering without pre-pressing and a green compact, powders used in ECAS can avoid binders. Since the powders densify while filling the cavity under applied pressure, moulds are made for the final part shape to prevent the issue of shape variations brought on by non-isotropic sintering and distortions brought on by gravity at high temperatures.

ii. Additive Manufacturing:

Metal powders (along with other materials, like plastics) are used in the additive manufacturing (AM) technology family to create parts through laser sintering or melting. As of 2015, this process is evolving quickly, therefore it's debatable whether to categorise it as a PM process at this time. Three-dimensional printing,

selective laser sintering, selective laser melting, and electron beam melting are examples of processes.

ii. (a) Foil diffusion bonding:

Metal foil layers are layered with long fibres and then pushed together to produce a matrix.

2.2.2 Methods involving liquids

i. Electroplating and electroforming:

Both electroplating and electroforming, which both rely on the electro-deposition process, are utilised in the production of metal products. The metal deposited in electroplating becomes a part of the surface it is deposited on, whereas electroforming produces a product that is distinct from the model. In contrast to electroplating, which only creates the product's outside layer, electroforming typically involves the complete creation of the product. A thin coating is applied to an object's exterior by electroplating, usually to improve its aesthetic or usefulness. Electroplating can be used to increase an object's hardness, corrosion resistance, conductivity, and a variety of other properties. The procedure can be used on a number of items, including electroforms, and different metals can be used for the plating.

ii. Stir casting

Discontinuous reinforcement is stirred into molten metal before it solidifies. A mechanical stirrer is used in the stir casting process to create a vortex that mixes the reinforcement with the matrix material. Due to its low cost, suitability for mass production, simplicity, nearly net shaping, and ease of composite structure control, it is an appropriate procedure for producing metal matrix composites. A furnace, reinforcement feeder, and mechanical stirrer make up a stir casting apparatus. The ingredients are heated and melted in the furnace. The bottom poring furnace is better suited for stir casting because instant poring is needed to prevent the solid particles from settling in the bottom of the crucible after stirring the combined slurry. In order to create the vortex that facilitates the mixing of the reinforcement materials added to

the melt, a mechanical stirrer is used. The impeller blade and the stirring rod make up a stirrer. The geometry and number of blades of the impeller blade might vary. As it leads to an axial flow pattern in the crucible with less power consumption, flat blades with three numbers are preferred. This stirrer is attached to motors with various speeds, and the regulator attached to the motor regulates the stirrer's rotational speed. The feeder is also connected to the furnace and is used to feed the reinforcing powder into the melting metal. The blended slurry can be poured into a permanent mould, sand mould, or lost-wax mould. The method of stir casting involves many processes. The matrix materials are maintained for melting in the bottom pouring furnace throughout this procedure. In order to remove moisture, impurities, etc., reinforcements are simultaneously warmed in a different furnace at a specific temperature. The feeder included in the setup is used to feed reinforcement particles at a constant rate into the centre of the vortex after the matrix material has melted at a specific temperature. The mechanical stirring process is then continued for a predetermined amount of time after the reinforcement particles have been completely fed. The molten fluid is then placed into a heated mould and left there to cool naturally and solidify. Additional post-casting procedures, including heat treatment, machining, testing, and inspection, have been carried out.

iii. Pressure infiltration:

Molten metal is infiltrated into the reinforcement using a type of pressure such as gas pressure.

iv. Squeeze casting:

Die casting and forging are combined in the casting process known as squeeze casting. A high-quality casting is created by starting with low pressure casting and then applying very high pressure when the material cools. A hydraulic press that is a component of the casting apparatus is frequently used for this. Squeeze casting was initially developed to produce metal components with greater strength for usage in the construction and defence sectors. This procedure produces metal parts that are more resistant to heat and wear, but they are historically highly expensive to make. The automotive and agricultural sectors are now included in the market for these

components. Spray deposition: A continuous fibre substrate is sprayed with molten metal.

v. Reactive processing:

A chemical reaction takes place, with one of the reactants producing the matrix and the other reinforcing it.

2.2.3 Methods based on semi-solid states

i. Semi-solid powder processing:

The powder mixture is heated to a semi-solid condition before being pressed to create the composites.

ii. Physical vapour deposition:

The fibre is passed through a large cloud of evaporated metal, which coats it.

2.2.4 Methods of in-situ fabrication

i. Controlled unidirectional solidification of a eutectic alloy can result in a two-phase microstructure with one of the phases spread in the matrix in lamellar or fibre form.

2.3 Hardness Measurement

Hardness is the ability of a material to resist local permanent or plastic deformation or indentation. Particularly in applications involving surface contact and relative motion of the component parts, material hardness is of significant and crucial significance. Surface wear is influenced by hardness, longevity and effectiveness of tribological systems and components. Due to their reduced weight and increased durability, metal matrix composites are growing in popularity. The distribution of hard particles in the soft matrix affects the uniform hardness of these materials. Hence, in Micro hardness testers, extremely low loads are used to assess the hardness of metallic composites.

Based on the indentation depth (d), bulk hardness of a material is typically classified into three types: Nano-hardness (d <1 μm), micro-hardness (d = 1-50 μm), and macro-hardness (d > 50 μm). Based on the material being tested, a suitable load is chosen to reach

the relevant indentation depth. Vickers hardness test is popular among researchers since it is simpler to execute. Moreover, neither the size of the indenter nor the applied load affect the hardness that is determined by this test. Furthermore, regardless of their hardness, different materials can be indented using the same indenter. In order to calculate the Vickers hardness number using this method, a square-based pyramidal diamond indenter is driven into the test surface. Once removed, the lengths of the two diagonals of the projected area of indentation are measured. In the Vickers test, the indentation time is constrained to 10 to 15 seconds while the applied force ranges from 1 gf to 120 kgf. After the load has been removed from the material, the two diagonals of the indentation left behind are measured under a microscope, and their average (d) is computed. The ratio F/A, where F is the applied force and A is the surface area of the indentation that results, determines the hardness number (HV).

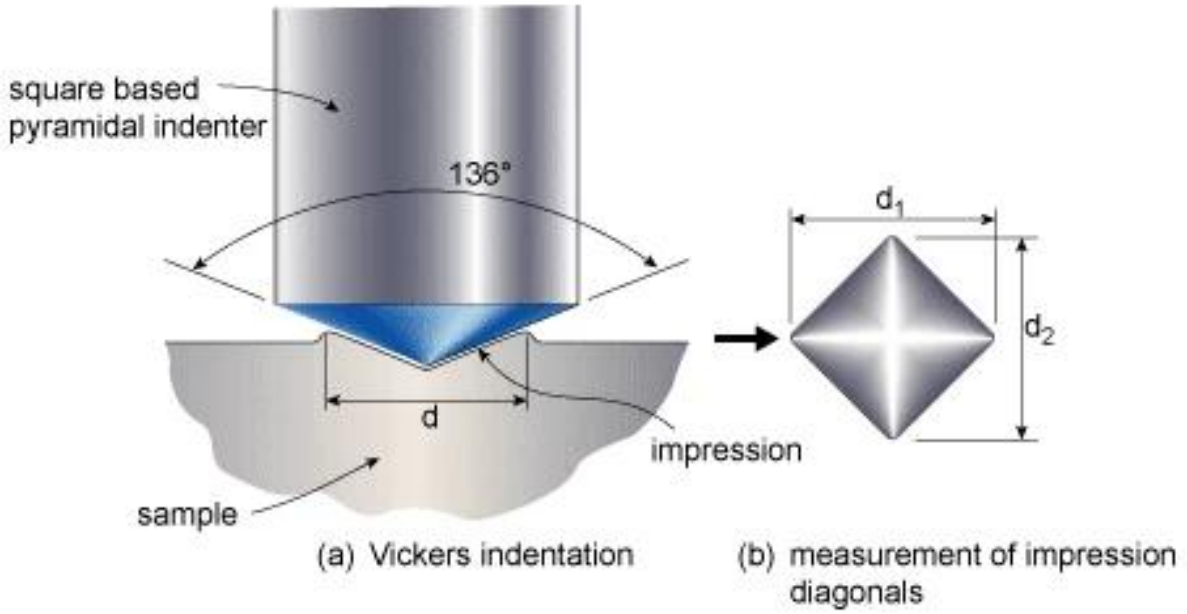

Figure 1.1 Vickers Hardness

The trigonometric formula shown below can determine 'A

$$A = \frac{d^2}{2\sin(\frac{136^o}{2})} = \frac{d^2}{1.8544}$$

In this study we used micro-Mach Technologies Micro hardness tester Model-MMVA, SR No.-133as per ASTM E384-17 standard.500 gf (gram force) load was applied with dwell time 20 seconds at 5 random places. Before the test samples were polished using SiC-2000 grit papers. Digital hardness data was shown via software that was attached to a hardness tester.

2.4 Tribological Testing

The main objective of this study is to determine the wear and friction characteristics of Al-RHA composites. For this we have done sliding wear test using Pin on Disc tribo-meter. The wear and friction force are influenced by several parameters like load, sliding speed, sliding distance, counter face material etc. Wear is a significant parameter to control losses for maintenance of equipment's in industries. So perfect evaluation of the impact of different factors are necessary. Pin on Disk tribo-meter was developed for measuring wear and friction. A counter-face disk which is harder than the sample was rotated against the sample pin. Sample pins are of dimension 3 mm diameter and 10 mm height. After each experiment the weight of the sample measured. Difference between the weight before experiment and weight after instrument is considered as wear. The counter disc material is made of EN 31 steel disc with hardness of 62 Hrc (Rockwell hardness).

2.5 Microstructure Characterization

Material characterisation of the composite is carried out to know the grain size, phase, distribution of the material. When a new material is fabricated, it must be characterised to ensure that the structure, chemical composition, distribution, and so on are exactly as desired. Furthermore, characterising a material allows us to better understand and explain its properties, physical behaviour, and performance from a specific perspective. Microscopic techniques are in high demand for material research and characterization. These techniques are very coherent and fast, allowing one to quickly determine the relationship between a material's properties and structure. As a result, it will aid in the development of new materials with novel property combinations. They also aid in determining whether a material has been properly heat treated. An effective method for closely examining a material's microstructure or surface morphology is scanning electron microscopy (SEM). This technique involves scanning a surface of a specimen to be examined with an electron beam, collecting the reflected (or back-scattered) beam of electrons, and then displaying the collected electrons at

the same scanning rate on a CRT (cathode ray tube) monitor or an LCD (liquid crystal display). It is possible to take pictures of the screen image that shows the specimen's surface characteristics. The specimen must be electrically conductive for SEM to work. With a significant depth of field, the SEM's magnification ranges from approximately from 10 to 50000 times.

2.5 Design of Experiment

Design of Experiment is a systematic approach to handle cost effectively all the parameters. This provides various information about the interactions of the parameters or factors. The term "design of experiments" (DOE) refers to a subfield of applied statistics that focuses on the planning, carrying out, analysing, and interpreting of controlled experiments to determine the variables that affect the value of a parameter or set of parameters. DOE is a potent instrument for data gathering and analysis that may be applied in a range of experimental settings.

It enables the manipulation of numerous input variables to ascertain how they affect a desired outcome (response). DOE can find significant interactions by adjusting several variables simultaneously that might be overlooked when experimenting with a single element at a time. It is feasible to study every conceivable combination (full factorial) or only some of them (fractional factorial). A carefully thought out and carried out experiment may reveal a lot about the impact of one or more factors on a response variable. In many experiments, some variables are kept constant while the amounts of another variable are changed. Yet, compared to altering factor levels simultaneously, this "one factor at a time" (OFAT) method of processing knowledge is ineffective. The work of R. A. Fisher in the early 20th century serves as the foundation for many of the current statistical methods for design of experiments. Fisher gave an example of how carefully planning an experiment design and execution before starting it might help analyse difficulties that are regularly faced. Blocking, randomization, and replication are essential ideas in designing an experiment.

2.5.1 Orthogonal Array

Design of experiments (DOE) is a method for getting the most useful data from the least amount of time, effort, money, or other finite resource. The DOE can cheaply complete tasks in the industries that include problem-solving and product/process design optimization.

Engineers and researchers can drastically save the time needed for experimental studies by understanding and using this technique. An orthogonal array (OA), based on the Taguchi approach, is used to minimise the number of experiments required to identify the ideal level combination of control parameters. An orthogonal array offers a continuous matrix of possible combinations in which all the parameters are changed to take into account both their direct effects and interactions. Many conventional orthogonal arrays have been tabulated by Taguchi. The choice of an appropriate OA design is essential to an experiment's success. It depends on the overall number of degrees of freedom needed to investigate both the primary effect and any interactions, the experiment's objective, the resources and funding available, and the time restrictions. The number of impartial and independent comparisons drawn from a collection of observations is referred to as the degree of freedom (DOF). In DOE, there are one fewer degrees of freedom (DOF) per factor than there are levels related to that factor. Moreover, the sum of the DOFs linked to each of the primary effects in an interaction equals the number of DOFs associated with that interaction.

The OA for a certain study is chosen in such a way that the quantity of experimental runs in the OA should exceed the total DOF necessary for reviewing the intended effects. Based on factors and their levels, there are numerous orthogonal array designs accessible. The choice of a suitable orthogonal array design is crucial for optimization because it cuts down on the time and expense of experimenting. L9 and L27 orthogonal arrays were available for analysis in the Minitab programme when it came to design factors and levels, but L27 orthogonal was chosen since it allows for factor interaction and increases analysis accuracy. The L27 Orthogonal array uses 13 columns and a total of 27 experimental runs (trail runs); each column is assigned to a factor in accordance with the needs of the study, and interdependent factors are arranged in this manner. The L27 Orthogonal array in its simplest version, which includes all 13 columns and 27 rows of experimental sets, is shown in Table 2.1.

2.5.2 Taguchi Method

In the 1950s, Japanese engineer and statistician Genichi Taguchi created the Taguchi method while constructing a telephone-switching system for the company Electrical Communication Laboratory. He wanted to raise the calibre of manufactured goods using statistics.

Table 2.1-Orthogonal Array

Trials	**1**	**2**	**3**	**4**	**5**	**6**	**7**	**8**	**9**	**10**	**11**	**12**	**13**
1	1	1	1	1	1	1	1	1	1	1	1	1	1
2	1	1	1	1	2	2	2	2	2	2	2	2	2
3	1	1	1	1	3	3	3	3	3	3	3	3	3
4	1	2	2	2	1	1	1	2	2	2	3	3	3
5	1	2	2	2	2	2	2	3	3	3	1	1	1
6	1	2	2	2	3	3	3	1	1	1	2	2	2
7	1	3	3	3	1	1	1	3	3	3	2	2	2
8	1	3	3	3	2	2	2	1	1	1	3	3	3
9	1	3	3	3	3	3	3	2	2	2	1	1	1
10	2	1	2	3	1	2	3	1	2	3	1	2	3
11	2	1	2	3	2	3	1	2	3	1	2	3	1
12	2	1	2	3	3	1	2	3	1	2	3	1	2
13	2	2	3	1	1	2	3	2	3	1	3	1	2
14	2	2	3	1	2	3	1	3	1	2	1	2	3
15	2	2	3	1	3	1	2	1	2	3	2	3	1
16	2	3	1	2	1	2	3	3	1	2	2	3	1
17	2	3	1	2	2	3	1	1	2	3	3	1	2
18	2	3	1	2	3	1	2	2	3	1	1	2	3
19	3	1	3	2	1	3	2	1	3	2	1	3	2
20	3	1	3	2	2	1	3	2	1	3	2	1	3
21	3	1	3	2	3	2	1	3	2	1	3	2	1
22	3	2	1	3	1	3	2	2	1	3	3	2	1
23	3	2	1	3	2	1	3	3	2	1	1	3	2
24	3	2	1	3	3	2	1	1	3	2	2	1	3
25	3	3	2	1	1	3	2	3	2	1	2	1	3
26	3	3	2	1	2	1	3	1	3	2	3	2	1
27	3	3	2	1	3	2	1	2	1	3	1	3	2

After experiencing success in his home Japan, Taguchi's theories started to acquire traction in the West by the 1980s, making him well-known in the United States. His strategies have been implemented by well-known multinational corporations like Toyota Motor Corp., Ford Motor Co., Boeing Co., and Xerox Holdings Corp.

The Taguchi approach is a useful tool for creating high-calibre systems. It presents a unified method for quickly and effectively determining the optimal selection of designs for quality, performance, and computational cost. Because it has been demonstrated to be highly effective in enhancing the quality of industrial products, this method has been widely used in engineering analysis to optimise performance behaviour within the combination of design parameters. The process or product should be designed in three steps for this optimisation technique: system design, tolerance design, and parameter design. The use of scientific and engineering knowledge necessary for part production is revealed by system design. Both the process design stage and the product design stage are included in this design. Materials, components, potential product parameter values, etc. are all chosen at the product design stage. Similar study of process sequences, equipment selection, provisional process parameter values, etc. are included in the process design stage. The parameter design is employed for the development of quality characteristics as well as for figuring out the ideal levels of process parameters and the values of the product parameters that result from the ideal levels of process parameters. It is anticipated that the values of the optimal process parameters determined by parameter design will be insensitive to changes in the environment's conditions and other noise-related elements. In order to attain excellent quality without raising the cost factor, parameter design is crucial in the Taguchi method. Finally, tolerances about the ideal combinations suggested by parameter design are resolved and analysed using the tolerance design. If the reduced variance produced by the parameter design falls short of the desired performance, tolerance design is necessary.

2.5.2.1 Signal to Noise Ratio

By calculating the average factor effect and subsequently identifying the ideal factor values (optimum condition), the findings are simply averaged. While being a very straightforward computation, the average does not account for the variation in outcomes within a trial condition. Using the mean squared deviation (MSD), which includes the average and standard deviation of the data, is a superior way to coordinate the behaviour of the variables. It is advised to analyse the results using a logarithmic transformation of MSD

known as the signal-to-noise (S/N) ratio in order to preserve linearity and contain a wide range of data. As a result, when the S/N ratio is employed for result analysis, the ideal situation that can be understood from such analysis is more just to provide more consistent performance. the terms "signal" and "noise" refer to the desired value (mean) and the unwanted value (standard deviation, or S.D.) for the output characteristic, respectively. As a result, the ratio of the mean to S.D. is the signal to noise ratio. The quality feature that deviates from the desired value is measured using the S/N ratio. The signal-to-noise ratio formulations for the three categories of quality characteristic are as follows: -

S/N ratio for SMALLER–THE–BETTER (minimize),

$$S/N = -10 * \log\left(\sum(y^2)/n\right)$$

S/N ratio for LARGER – THE – BETTER (maximize),

$$S/N = -10 * \log(\frac{1}{n}\sum(1/y^2))$$

S/N ratio for NOMINAL – THE – BEST,

$$S/N = 10 * \log(\bar{y}/S_y^2)$$

$\bar{y}$ is the average of the observed data (y), n is the number of observations, and S_y^2 is the variance of y. The decibel (dB) scale is used to express these S/N ratios. The Taguchi technique employs OA to minimise the quantity of tests required to identify the ideal process parameters. Taguchi has compiled a number of conventional orthogonal arrays. The success of the experiment depends on selecting the right OA. The purpose of the experiment, the resources and budget at hand, the amount of time available, and the overall degree of freedom needed to explore the main and interaction effects are all factors. By using a minimal number of experimental trials, orthogonal arrays enable one to ascertain the main factor and interaction factor implications.

2.5.2.2 Analysis of Variance

A statistical approach called analysis of variance can be used to locate and quantify the causes of variation within a set of data. By segmenting the entire variation data and comparing each segment to the overall variation, variance analysis is performed. ANOVA

also aids in establishing whether changes are brought on by variance within or between approaches. Individual diversity among treatment groups causes the within-method variations, whereas method differences cause the between-method variances. So, in general, ANOVA aid in identifying which process parameters have a significant impact on a system's performance.

2.5.3 Grey Relational Analysis

Huazhong University of Science and Technology's Deng Julong created the Grey Relational Analysis (GRA). It is one of the most often applied grey system theory models. GRA employs a certain idea of information. It categorises situations when there is incomplete information as black and complete information as white. But in actual problems, neither of these idealistic scenarios ever happens. In fact, the middle ground, when there is just partial knowledge, is referred to as being grey, hazy, or fuzzy. The Taguchi-based GRA model, a variation of the GRA model, is a well-liked optimization technique in production engineering.

The GRA is simply included into algorithms. The normalisation of response variables and determination of the Grey relational grade serve as the foundation for the Grey relational analysis. For the desired outcome, an analysis is carried out utilising the grey relational grade as the response variable. Confirmation tests are then carried out to verify the findings.

The linear normalisation of the experimental results in the range of 0 and 1 is the first step of the grey relational analysis. A grey relational generation is another name for this. Three goals can guide the normalisation process, which includes:

(1) Normalisation by maximum value or the higher-the-better standard (for example, profit)

$$X_i(k) = \frac{y_i(k) - \min y_i(k)}{\max y_i(k) - \min y_i(k)}$$

(2) Normalisation using the minimum value or the lower-the-better (for instance, a fault)

$$X_i(k) = \frac{\max y_i(k) - y_i(k)}{\max y_i(k) - \min y_i(k)}$$

(3) Normalization for nominal is the best

$$X_i(k) = \frac{\|y_i(k) - y_o\|}{\max y_i(k) - y_o}$$

Whereas min $y_i(k)$and max $y_i(k)$are the smallest and largest values of $y_i(k)$, and for the kth response, y_o is the targeted value, $X_i(k)$ is the value obtained after the grey relational generation. The perfect order is$X_o(k)$ (k=1, 2,..., n). When performing a grey relational analysis, the term "grey relational grade" refers to the degree of relationships between the 27 sequences [$X_o(k)$ and $X_i(k)$, where i = 1, 2,..., 27 and k = 1, 2,..., n].

To describe the link between the ideal (best = 1) and the actual experimental findings, grey relational coefficients are computed. Calculating the Grey relational coefficient$\xi_i(k)$ is as follows:

$$\xi_i(k) = \frac{\Delta_{min} + r\Delta_{max}}{\Delta_{oi}(k) + r\Delta_{max}}$$

Where Δ_{oi} = $X_o(k)$- $X_i(k)$= difference of the absolute value between $X_o(k)$ and $X_i(k)$, Δ_{min} and Δ_{max} are the minimum and maximum difference values of the absolute differences Δ_{oi} of all comparing sequences, and r is the distinguishing coefficient that is used to adjust the difference of the relational coefficient; typically, r falls within the .The separating coefficient lessens the impact of Δ_{min} The assumed value of the distinguishing coefficient, r, is 0.5 due to the moderate differentiating effects and good outcome stability when it becomes too large and enlarges the different significance of the relational coefficient. So, for purposes of further analysis in the thesis, r is taken to be 0.5.

The grey relational grade in the analysis reveals how the series are related to one another. The evaluation of the overall qualities of multiple responses is based on the grey relational grade, which is just the average of the grey relational coefficients produced in the preceding phase.

$$\alpha_i = \frac{1}{n}\sum_{k=1}^{n} \xi_i(k)$$

where n is the total number of performance traits. The experimental value $X_i(k)$and the ideal normalised value $X_o(k)$are more closely aligned the higher the grey relational grade. As was already indicated, the best procedure outcome in the experimental set is the ideal

sequence $X_o(k)$. A higher grey relational grade denotes a closer proximity to the ideal for the coinciding parameter combination.

In GRA, the numerical values of the grey relational grades between items have little practical significance, whilst the grey relational ordering produces more ambiguous data. The combination yielding the minimal grade is given the lowest order, and the combination generating the greatest grey relational grade is given an order of 1.

2.6 Closure

The fundamental theoretical issues are covered in this chapter. Different types of fabrication techniques are briefly discussed at beginning. The theoretical underpinnings of tensile, hardness, and tribological testing are then discussed. Finally, background information on the experimental design—one of the analytical methods—used in this study is provided. Within the design of experiments, the theory underlying the Taguchi method and Grey relational analysis is also covered.

Chapter 3

Experimental Details

3.1 Introduction

An experiment is described as a test or a series of tests in which significant modifications are made to a system or process input response in order to investigate and pinpoint the causes of potential changes in the output response. The most efficient and scientific way of all is discovered to be the experimental method. It is possible to make clear and significant inferences through careful preparation and implementation of an experiment, which improves how people perceive nature. The experimentation plan necessary for the current work is mentioned in the current chapter. Additionally, this chapter also covers the stir casting procedure that was employed to create the composite for the current investigation.

3.2 Density and Chemical Composition

The density of an Al-RHA (Aluminium-Rice Husk Ash) composite exhibits variability depending on the specific combination of materials and the processing methods applied. To accurately determine the density of a particular Al-RHA composite, rigorous experimental procedures are necessary, involving the measurement of its mass and volume through appropriate techniques like Archimedes' Principle or the Pycnometer Method. During the fabrication of the composite, the proportion of aluminium and rice husk ash used in the mixture plays a crucial role in determining the final density. The relative contribution of each component influences the packing arrangement and overall mass per unit volume, thus affecting the composite's density.

Table 3.1- Density of AL6061 and Rice Husk Ash

Sl No.	Material Name	Density g/cc
1	Al6061	2.6
2	Rice Husk Ash	0.34

Table 3.2 Chemical composition of Al6061

Chemical Element	Compositions (wt%)
Manganese (Mn)	0.0 - 0.15
Iron (Fe)	0.0 - 0.70
Magnesium (Mg)	0.80 - 1.20
Silicon (Si)	0.40 - 0.80
Copper (Cu)	0.15 - 0.40
Zinc (Zn)	0.0 - 0.25
Titanium (Ti)	0.0 - 0.15
Chromium (Cr)	0.04 - 0.35
Other (Each)	0.0 - 0.05
Others (Total)	0.0 - 0.15
Aluminium (Al)	Balance

Table 3.3- Chemical Composition of Rice Husk Ash

Chemical Element	Compositions (wt%)
Carbon dioxide	0.10
Calcium oxide	1.01
Silicon dioxide	89.90
Aluminium oxide	0.46
Iron oxide	0.47
Magnesium dioxide	0.14
Potassium oxide	4.50

3.3 Measurement of hardness

The characteristic of a substance that allows it to withstand being damaged is called hardness when a load is applied, another material causes permanent deformation. The testing of hardness is to quantitatively assess a material's resistance to plastic deformation. How hard it is based on the measurement of the indentation made on the test's surface samples. The widely utilised method is the Vickers test because of its wide load range capabilities. The

created samples that will be examined in this work include variation. when measuring the Micro hardness of reinforcing material in volume fraction,

3.4 Measurement of Friction and Wear

The Pin on Disk Multi Tribotester was used to conduct the tribological test. On a disc, pin device depicted in Figure 3.8. It is utilised to gauge the tribological properties of composite samples when they are lubricated using SAE20W40 and at room temperature. To prepare wear samples of the proper size, the casting pin is cut and machined appropriately (3mm x 10mm). The samples are pushed against a rotating steel disc constructed of EN31 steel with a hardness of 62 HRc (Rockwell Hardness). The standard dimensions of the samples are 3mm x 10mm. Before and after each run, the wear samples were washed with Acetone to get rid of any wear particles that had adhered to them. Composite samples are made to slide against the rotating disc while being maintained stationary by the attachment during the test. A computer connected to the tribo-tester can be used to regulate the speed of the disc and the length of tests. Dead weights placed on the loading pan and a loading lever are used to apply loads. The typical load sensor is close to the loading lever, which makes it easier to measure the actual load placed on the specimen. The frictional force sensor measures the frictional force and plots it in real-time on the computer screen using a beam-type load cell with a 1000 N capacity. It should be mentioned that wear is assessed measuring weight of the sample before and after the test. The disc material, however, experiences less wear than the composite sample because the hardness of the composites is substantially lower than the hardness of the disc material. Wear is typically quantified as a volume or mass loss. Wear in this situation is described in terms of wear in gm.

The values of the testing parameters will be reported in the chapters for the related studies in this thesis for the tribological studies pertaining to the variation of the tribological conditions. It should be mentioned that the components and their weights were selected based on manual studies, loading conditions discovered in many research publications, and methods employed by various researchers for the tribological studies of Al- RHA composites.

3.5 Selection of Orthogonal Array

By adjusting the controllable parameters, the current work seeks to investigate and optimise the tribological properties of Al-RHA metal matrix composites. The tribological

testing parameters are the factors that can be controlled in this investigation. For each of the factors, three levels with equal spacing within the operational range of the parameters were chosen. The use of three levels allows for the possible examination of curvature or nonlinearity effects. Volume fraction (V), applied load (L), and sliding speed are the tribological testing parameters (S). These parameters' (V, L, and S) interactions are also taken into account. Each of the primary components in the current situation is connected to a three-level. Each factor's DOF is 2, whereas the interaction's would be 4 (2× 2). The three major parameters (V, L, and S) will have a total of 6 degrees of freedom (3×2 DOF), while the three interaction effects (V, L, and) will have a total of 12 degrees of freedom (3×4 DOF). A total of 18 degrees of freedom (6 degrees + 12 degrees) would be present. As a result, L27 OA, which has 27 trials, was a good choice for this experiment. The factors (V, L, and S) and their interactions (VL, VS, and LS) are assigned to the columns of the chosen OA in accordance with the triangular table for three-level orthogonal array. The cell values in each row and column represent an experimental run and the factor settings for that run, respectively. Volume fraction (V), applied load (L), and sliding speed (S) are each assigned a column in the array, with the remaining columns being used to represent the two-way interactions between the factors and error terms. The main factor columns' cell values (V, L, and S) correspond to their levels (1, 2, and 3), whereas the same values for the interaction represent the sum of the levels of the main factors. For instance, column 3 and column 4 represent the interaction between V and L (VL), and the relevant cell for trial 1 displays 1 in column 3 and 1 in column 4. Because interaction VL has a value of 11, it combines levels 1 of A and B. There are nine such combinations for VL interactions in columns 3 and 4 (11, 22, 33, 12, 21, 23, 32, 13, and 31). ANOVA is used to calculate the % contribution of the interaction columns and error columns to the overall effect.

3.6 Study of Microstructure

In order for composite materials to operate well, microstructure is crucial. The microstructure, shape, size, and distribution of reinforcing particles in the alloys all affect the material's physical properties. Nothing can replace observing a uniform distribution of reinforcement throughout the composite. The uniform distribution of the reinforcing particle in a composite can be greatly revealed by microstructural analysis of the composite. It is crucial to establish factors such grain size, the alignment of the ceramic reinforcement's grains, the existence of inclusions, and voids in order to examine the composite samples. In a

typical microstructure analysis of a composite, the following key characteristics should be looked for: I the reinforcement's grain structure and alignment; (ii) the ceramic reinforcement's homogenous distribution; (iii) the research of the wear mechanism; and (iv) the impact of heat treatment. The majority of the time, using a variety of microscopy techniques, such as optical microscopy and scanning electron microscopy, will be necessary for practical micro-structural evaluation. This work makes use of a scanning electron microscope. Images of composite samples at magnification levels (100x, 250x, 500x, and 1000x) were taken using SEM and used for the investigation. This particular investigation was carried out to investigate the wear mechanism by analysing the microstructure of the composite wear tracks.

3.7 Closure

The experimental techniques employed for the current investigation are presented in this chapter. Initially, a thorough discussion of the manufacture of the Al- RHA composite is presented. Tensile strength, hardness, friction, and wear testing procedures are explained along with specifics on the testing equipment. The details of the microstructure study's equipment are then given.

Chapter 4

Results of the Experiment

4.1 Introduction

The main motivation behind using Agro -Waste as reinforcement in Al6061 is to improve its tribological and mechanical behaviour. Fabrication process used for this study is stir casting. Two main tribological behaviour is friction and wear. Friction reduces efficiency of a mechanical devices which are in relative motion. Wear is responsible for reduction in service life of mechanical components. So our objective is to minimize both wear and friction. We also studied hardness property of Al-RHA composite as hardness is co-related to wear. The easiest way to reduce wear is use of lubrication there are different types of lubricant used in mechanical assembly. For this research work we used SAE-20W40 as lubricant. Lubricant were applied with 6 kg/cm² pressure.

In this chapter mechanical property such as hardness is and furthermore optimization of friction and wear data is done using Taguchi method. Multi-response optimization is done using GREY (Grey Relational Analysis) to find optimum combination for friction and wear characteristics.

4.2 Micro structure

After fabricating the Al-RHA composite its microstructure was studied. The size of the specimen was given as per the necessity for different techniques. We have carried out optical microscopy and scanning electron microscopy for this purpose.

Microstructure of Al-RHA samples were observed in 200X magnification and it is shown in Figure 4.1.

The optical microstructure of the Al6061-RHA composite is shown in Figure 4.1. confirmed that there was a homogeneous distribution of RHA particles in the base matrix of Al6061 alloy and demonstrated the presence of RHA particles in the matrix.

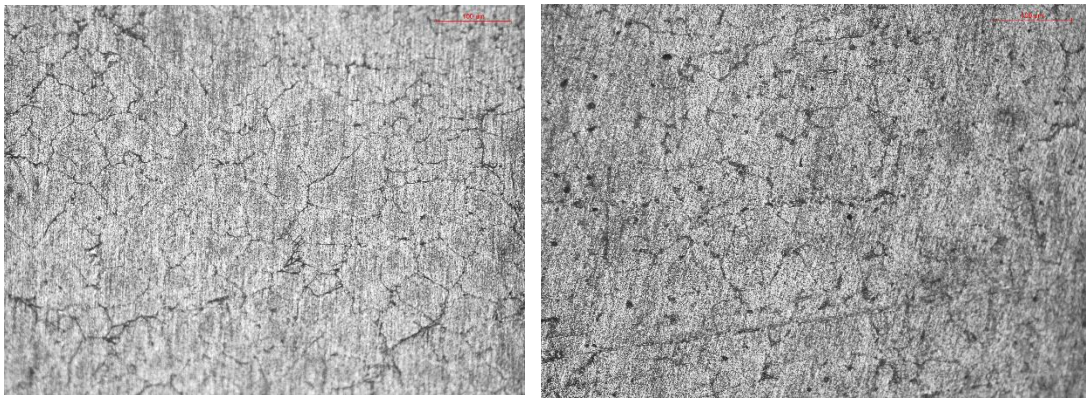

(a) **(b)**

(c)

Figure 4.1 -a)Optical micrograph ofAl-4%RHA
b)Optical micrograph of Al-8%RHA,
c)Optical micrograph of Al-12 %RHA at 200X magnification

4.2.1 SEM Analysis of Fabricated composite

In Figure 4.2 the SEM images of the Al6061-RHA composite exhibit that there were no voids or discontinuities in the composite. Also Figure 4.2 clearly demonstrates that there was good interfacial bonding between the RHA particles and matrix components and there is no agglomeration of reinforcement particle found in the composite.

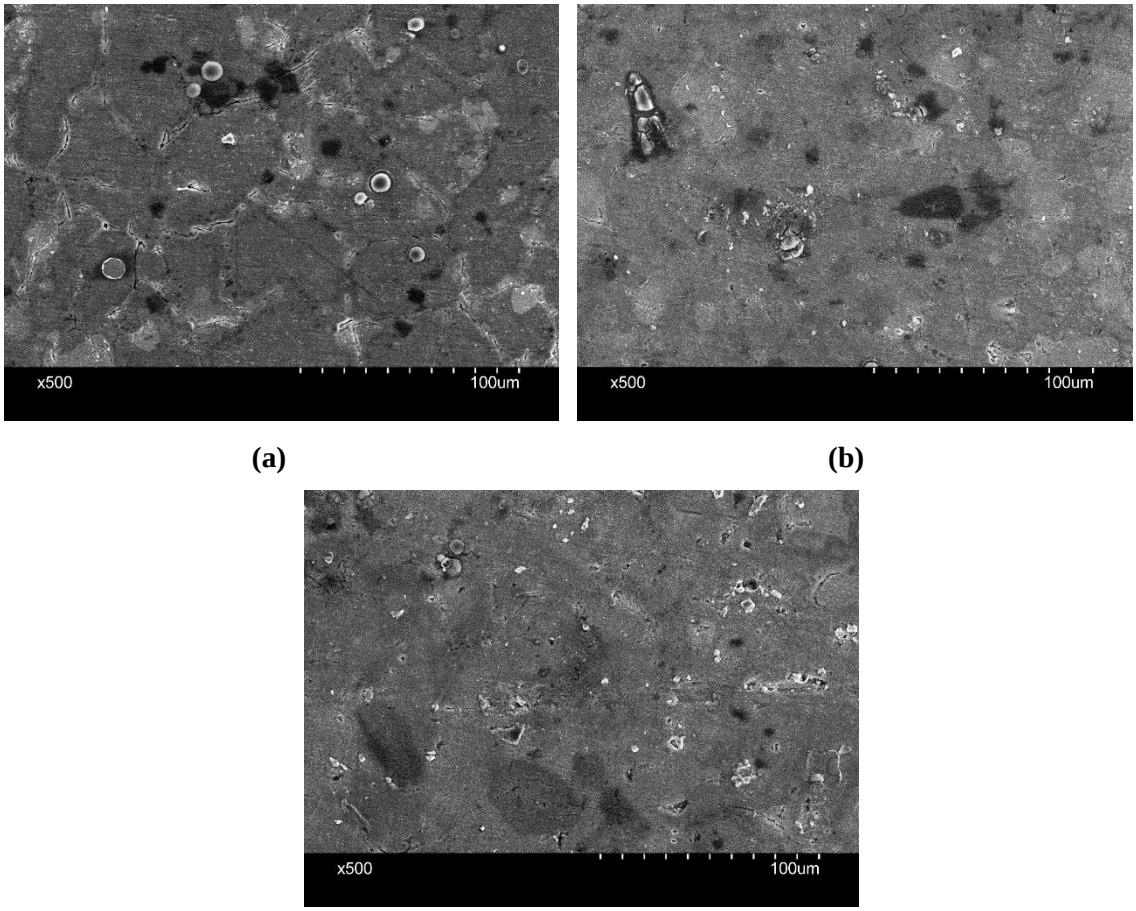

(a) **(b)**

(c)

Figure 4.2 SEM image of a) Al6061-4 %RHA,
b) Al6061-8 %RHA,
c) Al6061-12 %RHA at 500X magnification

4.3 Micro hardness

Micro hardness study of Al-RHA composite is measured using Vickers Micro hardness tester. Before testing composites were cleaned to remove scratches and dirt's. Each test was repeated 5 times and average values were tabulated in Table 4.1. The Hardness values are represented using a bar chart in the Figure 4.3.

From the study it can be concluded that hardness value increased from 70.9 VHN to 75.5 VHN when volume% (V) of rice husk incremented from 4% to 12 %. The strain energy increases in the perimeter of the particles in the matrix as a result of the addition of particles to the matrix, which is related to the hardening behaviour of composite materials.

Table 4.1 Hardness value of Al6061-RHA composites

Sample No.	Composite	Hardness (VHN)
1	Al6061+4 %RHA	70.9
2	Al6061+8 %RHA	73.5
3	AL6061+12 %RHA	75.5

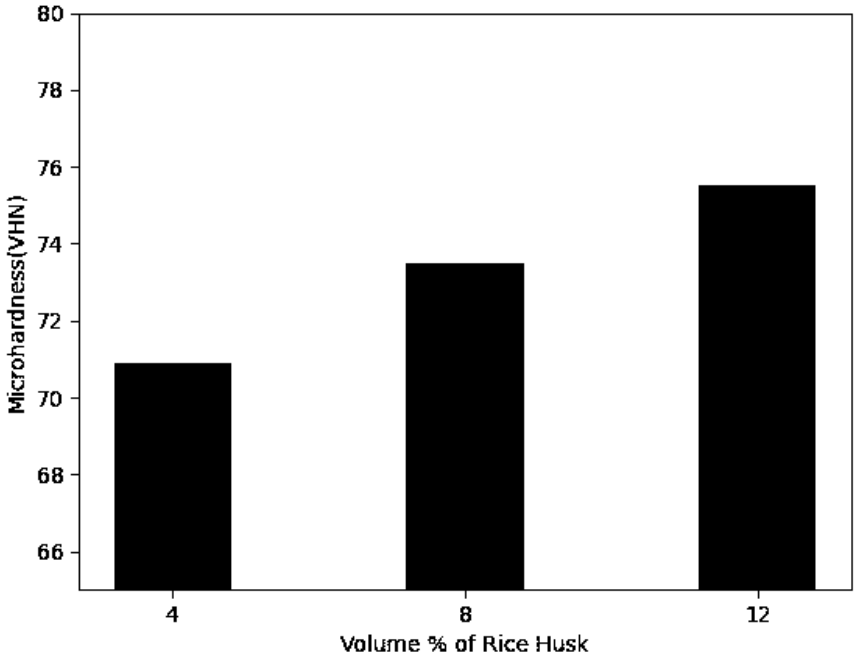

Figure 4.3 Hardness Value of Al6061-RHA composite

4.3 Analysis of Experiment

The current chapter examines the optimisation of wear and friction properties separately and jointly. The combination of design parameters for each experiment is chosen using the Taguchi L27 orthogonal array (OA) for the optimisation of friction and wear. Table 4.2 lists the design parameters and their values at various levels. The Taguchi method is then used to examine the trial data in order to determine the ideal combination of design parameters, where friction and wear are both reduced to the absolute minimum. Similar procedures are used for the multiple response optimisation. The friction and wear

experimental results are transformed to a Grey relational grade. In prior chapters, the method for creating Grey relationship grades is discussed. The ideal combination of design parameters is then produced using this Grey relational grade and Taguchi approach. An analysis of variance (ANOVA) is carried out to determine the importance of each design parameter on the relevant response. The confirmation test is necessary to see how various responses change from the initial combination of design parameters to the final combination.

Table 4.2 Parameters used in the Experiment

Levels	Design Factors		
	Volume%	**Load(N)**	**Sliding Speed(m/s)**
1	4	10	2
2	8	20	3
3	12	30	4

4.4 Frictional Study

Stir cast Al-RHA metal matrix composite's friction behaviour is investigated and optimised. The response variable for the optimisation analysis is the coefficient of friction (COF). Through the friction force sensor, the coefficient of friction values is obtained from the tribo tester. The coefficient of friction values are then calculated by dividing the frictional force values by the normal load. Table 4.3 provides the S/N ratio numbers and the coefficient of friction values for each trial. Since friction should be kept to a minimum, smaller-is-better criteria are used in the S/N ratio calculations.

It is possible to assess the importance of each process parameter based on the delta value provided in the response table.

Table 4.3 CoF and S/N Ratio of CoF data from experiment

Exp No.	Co-efficient of Friction	S/N Ratio
1	0.157	16.0820
2	0.174	15.1890
3	0.243	12.2879
4	0.202	13.8930
5	0.223	13.0339
6	0.191	14.3793
7	0.199	14.0229
8	0.266	11.5024
9	0.229	12.8033
10	0.168	15.4938
11	0.178	14.9916
12	0.174	15.1890
13	0.208	13.6387
14	0.233	12.6529
15	0.177	15.0405
16	0.175	15.1392
17	0.256	11.8352
18	0.186	14.6097
19	0.207	13.6806
20	0.145	16.7726
21	0.256	11.8352
22	0.159	15.9721
23	0.166	15.5978
24	0.253	11.9376
25	0.212	13.4733
26	0.191	14.3793
27	0.257	11.8013

Table 4.4 Response table for S/N ratio of CoF

Level	Volume	Load	Sliding Speed
1	13.69	14.61	14.60
2	14.29	14.02	13.99
3	13.94	13.29	13.32
Delta	0.60	1.33	1.28
Rank	3	1	2

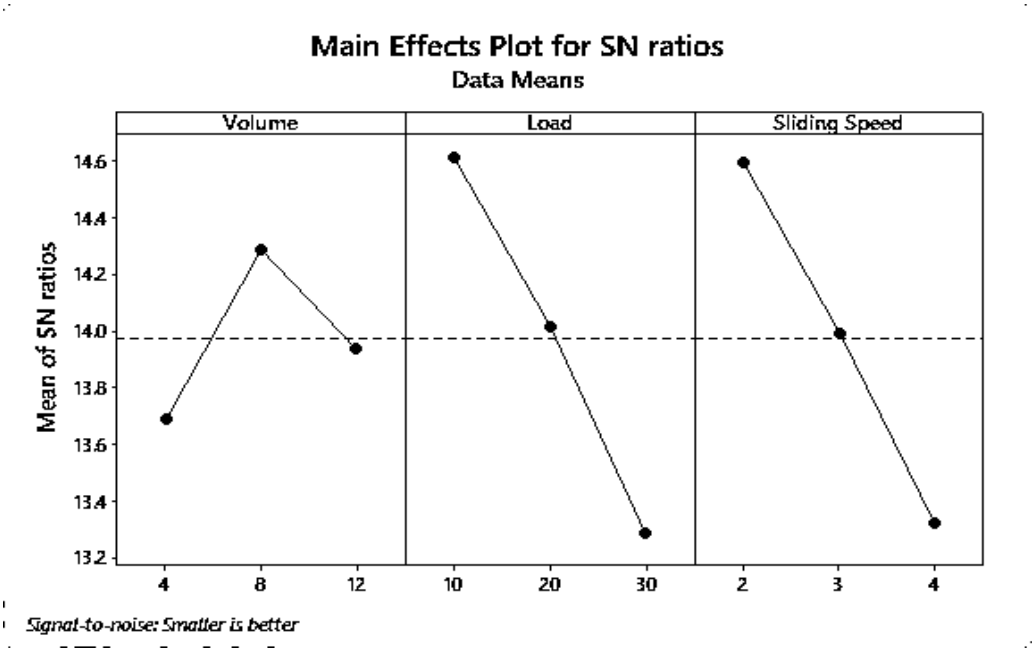

Figure 4.4 Main Effect plot of S/N ratio of CoF

According to the response table for the S/N ratio for COF (Table 4.4.), a factor's rank is determined by its delta value; rank 1 is given to the factor with the greatest delta value, rank 2 to the factor with the second highest value, and rank 3 to the factor with the third highest value. The biggest delta value in this case is for the parameter load (L), followed by sliding speed (S) and volume fraction (V).

The S/N ratio value is clearly higher at level 2 for volume fraction (V), level 1 for load (L), and level 1 for sliding speed (S) parameters, as seen in Figure 4.4. Therefore, V2, L1, and S1 are the ideal combinations. For a minimum COF of Al-RHA, V2L1S1 (i.e., Volume

fraction = 8 %, Load = 10 N, and Sliding speed = 2 m/s) is the ideal setting for the control parameters.

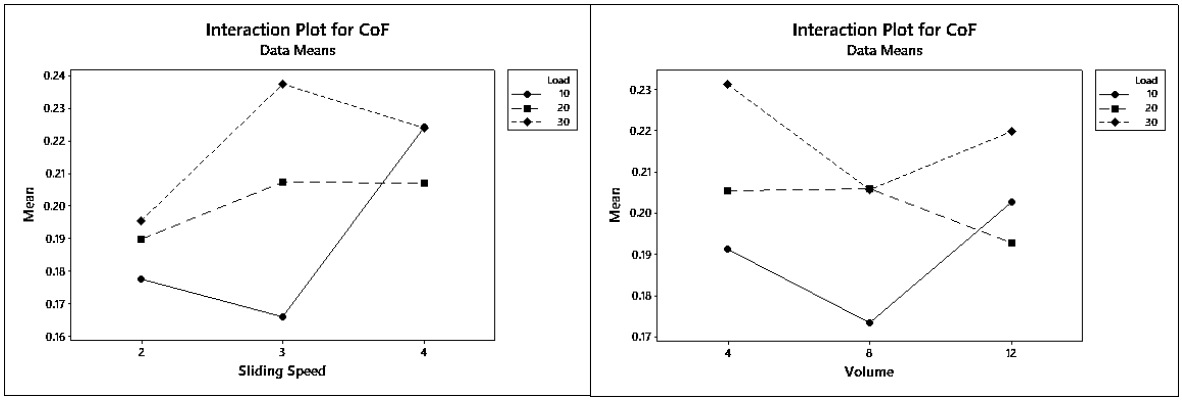

(a) **(b)**

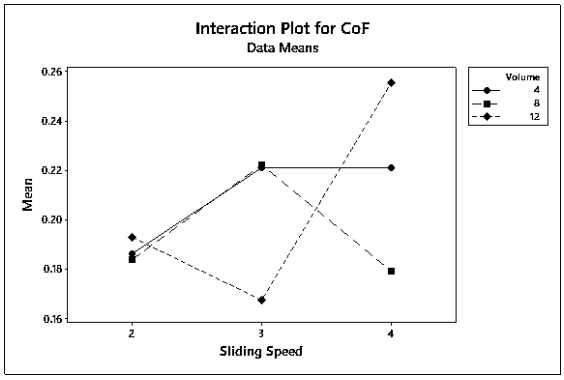

(c)

Figure4.5 Interaction plot for S/N ratio (a) Sliding Speed Vs Load, (b) Volume Vs Load, (c) Sliding Speed Vs Volume

Figures 4.4 and Figure 4.5 display the main effects and interaction effects plots between the process parameters. The slope of the main effects plot indicates the importance of each component. The parameter that has the most impact on the line's inclination will be that one. The main effects plot makes it abundantly evident that parameter L (load) is the most important parameter, followed by parameter S (slide speed), and parameter V (volume fraction) also has some substantial effects. Analysing an interaction plot helps in figuring out whether parameter effects are not parallel. When the lines of an interaction plot are not parallel, it indicates that there has only been nominal interaction, and when the lines cross, there have been significant interactions between the parameters. The interaction between the parameters S and L and S and V is high, as shown in Figures 4.5, whereas the interaction between the parameters L and V is mild. Therefore, it is evident from the current analysis that the load (L) is the most crucial parameter for the friction properties of Al-RHA metal matrix

composites. The process parameter sequence that produces the highest mean S/N ratio is found to be V2L1S1, and the same is true for the lowest friction coefficient. The analysis of variance test was used to identify the crucial variables and their interactions with the composite Al-RHA sample data. Each factor's % impact on AL-RHA as well as its interactions with other factors are assessed.

Table 4.5 ANOVA data for CoF

Source	DF	Adj SS	Adj MS	F-Value	P-Value	Contribution %
Volume	2	0.000977	0.000488	1.17	0.358	2.95%
Load	2	0.004065	0.002032	4.88	0.041	12.29%
Sliding Speed	2	0.004327	0.002163	5.19	0.036	13.08%
Volume*Load	4	0.001668	0.000417	1.00	0.460	5.04%
Volume*Sliding Speed	4	0.013831	0.003458	8.30	0.006	41.82%
Load*Sliding Speed	4	0.004873	0.001218	2.93	0.092	14.74%
Error	8	0.003332	0.000416			10.07%
Total	26	0.033071				100.00%

ANOVA is a statistical method for the study of experimental data. This technique is particularly helpful for demonstrating the degree of significance or the influence of a factor or factors and their interactions on a certain response. It breaks out the contribution of each element and the mistake to the overall response variability. To ascertain which parameter and interaction genuinely effect the performance characteristics, an ANOVA is conducted using Minitab 17 Version. Table 4.5 presents the analysis of variance (ANOVA) findings. The F-ratio, or ratio of regression mean square to mean square error, is calculated by the ANOVA. The F ratio, also known as the variance ratio, is the comparison between the variance brought on by a factor's effects and the variance brought on by the error term. This ratio is used to

assess how the parameters under study affect the variance of all terms included in the error term at the specified level of significance, generally speaking, as the F value rises, so does the parameter's importance. The percentage contribution of each parameter is displayed in the ANOVA table. According to the table, the most important parameter is Sliding Speed(S), which contributes 13.08%. Among the parameters that affected interactions, load (V) vs. sliding speed (S) contributed 41.82%.

A multiple regression model was applied using statistical programme "MINITAB" for confirmation. According to this model, the relationship between factors and a response variable was fitted to the observed data as a linear equation. As a result, a relationship between the significant terms from the ANOVA analysis volume fraction, load, sliding speed, and their interactions is established in the regression equation.

The regression equation for CoF-

CoF = 0.010833S + 0.0040028L - 0.00045833LS - 0.0028819V + 0.0017292VS - 0.00014167VL + 0.12231

The S/N ratio regression equation that was created is-

S/N Ratio = -0.555994S - 0.172761L + 0.0210267LS + 0.112208V - 0.0630104VS + 0.00540792VL + 17.5825

Table 4.6 Confirmation test data for COF

Sl No	V	L	SS	COF	S/N Ratio	CoF (From eq)	S/N ratio (From eq)	Diff in CoF	Diff in S/N ratio
1	4	10	2	0.157	16.0820	0.171	15.3245	0.015	-0.6575

The results of the confirmation test are displayed in Table 4.6 along with a comparison to the multiple regression model under ideal conditions. The computed values and experimental values were created using the regression model. The experiment's S/N ratio values come out to differ from those predicted by the regression equation by a difference of

0.6575. The computed S/N ratio value derived from the equation of the regression model and the experimental data are almost identical with little variation.

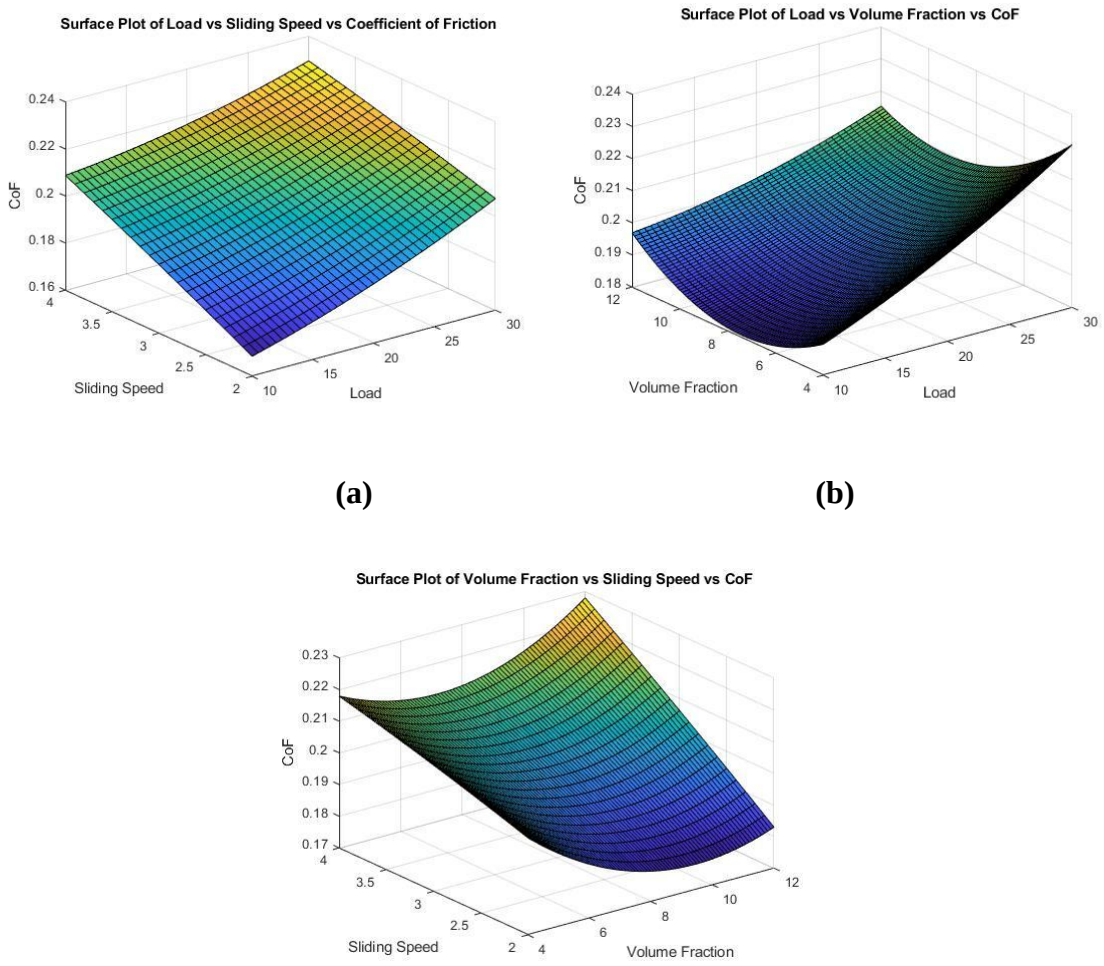

Figure 4.6 Surface plot for (a) Load vs Speed vs CoF ,(b) Volume fraction vs load vs CoF, (c)Sliding Speed vs Volume Fraction vs CoF

To comprehensively assess the influence of individual parameters on the wear and friction characteristics of the Al-RHA metal matrix composite, a detailed analysis is conducted. To aid in this analysis, surface plots are generated, providing valuable visual representations of the composite's behavior under different conditions. Surface plots are three-dimensional graphical representations that showcase the variations in wear and friction performance across multiple parameters. Each axis of the surface plot corresponds to a specific parameter, such as Sliding Speed (S), Load (L), or Volume Fraction (V), while the height of the surface represents the corresponding wear or friction response. By visualizing the surface plot, researchers and engineers can readily identify the trends and interactions

among different parameters, helping to pinpoint the optimal operating conditions for desired wear and friction characteristics.

Figures 4.6(a),4.6(b),4.6(c) are surface plots with contour lines that depict how the coefficient of friction varies as various parameter values change. The regression equations were utilised in Matlab software to produce the surface plots.

The surface plot is generated once the final two parameters are changed. The value of COF is determined by the interaction of the design variables, load, speed, and volume fraction of reinforcement. It is feasible to identify the location where the coefficient of friction will be lowest using these kinds of surfaces plots. It can be seen that the coefficient of friction value varies monotonically with variation in sliding speed in Figure 4.6's surface plot. Additionally, the COF value varies monotonically for the combination design factors sliding speed vs. volume fraction and sliding speed vs. applied load. The efficiency of the reinforcement is greater when applied load vs. sliding speed than when parameter volume fraction is used. The surface plot findings are matched by the best set of parameters for this, i.e., V2L1S1, which has the lowest coefficient of friction.

4.5 Wear Study

Table 4.7 presents essential wear data for the Al-RHA metal matrix composites, which is a key aspect of the current study. In this investigation, wear depth is chosen as the primary performance metric for the S/N (Signal-to-Noise) ratio analysis. The objective of the study is to minimize wear, making the "smaller-is-better" criterion the appropriate approach to evaluate the composite's performance in terms of wear resistance. By utilizing the S/N ratio analysis, the study aims to identify the optimal combination of parameters that results in the least wear depth. The S/N ratio figures provided in Table 4.7 offer valuable insights into the relative performance of different composites under varying conditions. A higher S/N ratio indicates better wear performance, implying that the composite exhibits reduced wear depth, which aligns with the study's objective.

The average values of each parameter at each level are listed in the response table (Table 4.8).

Table 4.7 Wear and S/N ratio data from experiment

Exp No	Wear	S/N ratio
1	0.0004	67.9588
2	0.0010	60.2199
3	0.0010	60.4455
4	0.0007	63.5218
5	0.0010	60.0727
6	0.0012	58.2966
7	0.0010	60.1460
8	0.0011	59.1066
9	0.0013	57.8332
10	0.0003	69.5424
11	0.0003	70.2196
12	0.0004	67.2636
13	0.0006	64.4370
14	0.0008	62.2140
15	0.0009	60.4455
16	0.0009	61.2430
17	0.0010	59.6454
18	0.0013	57.6105
19	0.0014	56.9746
20	0.0004	67.0981
21	0.0003	71.4806
22	0.0004	68.3285
23	0.0004	67.7797
24	0.0008	61.5836
25	0.0008	61.9382
26	0.0006	64.0824
27	0.0010	60.0000

Table 4.8 Response Table for Wear

Level	Volume	Load	Sliding Speed
1	60.84	65.6900	63.79
2	63.62	62.9600	63.38
3	64.36	60.1800	61.66
Delta	3.52	5.5100	2.13
Rank	2	1	3

From the response table we came to know Load (L) has the highest delta so it has given rank 1 followed by Volume % (V) and Sliding Speed (S).

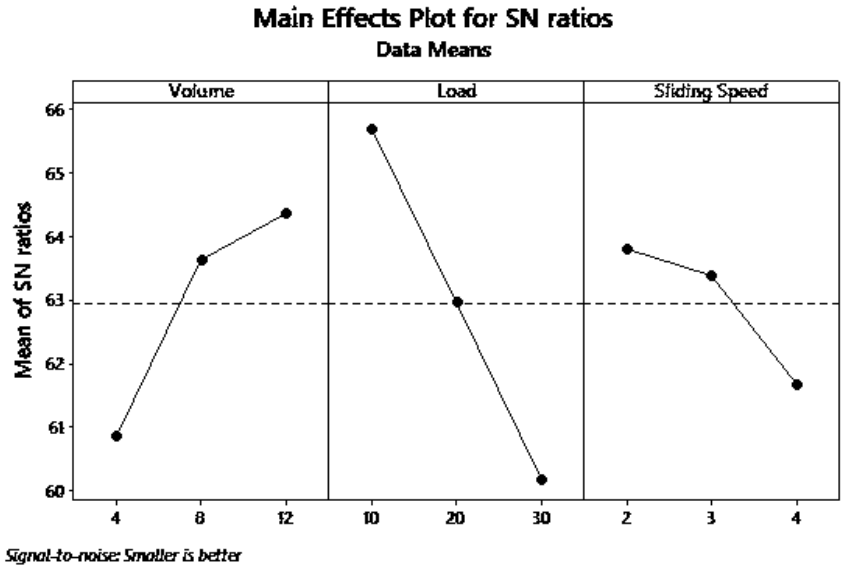

Figure 4.7 Main effect plot for S/N ratios for Wear

From main effect plot for Volume of Level 3 has highest S/N ration in case of load it was level 1 and for sliding speed it is level 1.so we can say V3L1S1 is the ideal combination of control parameters.

Figures 4.7 and 4.8 display the main effects and interaction effects plots between the process parameters. The slope of the main effects plot indicates the importance of each component. The parameter that has the most impact on the line's inclination will be that one.

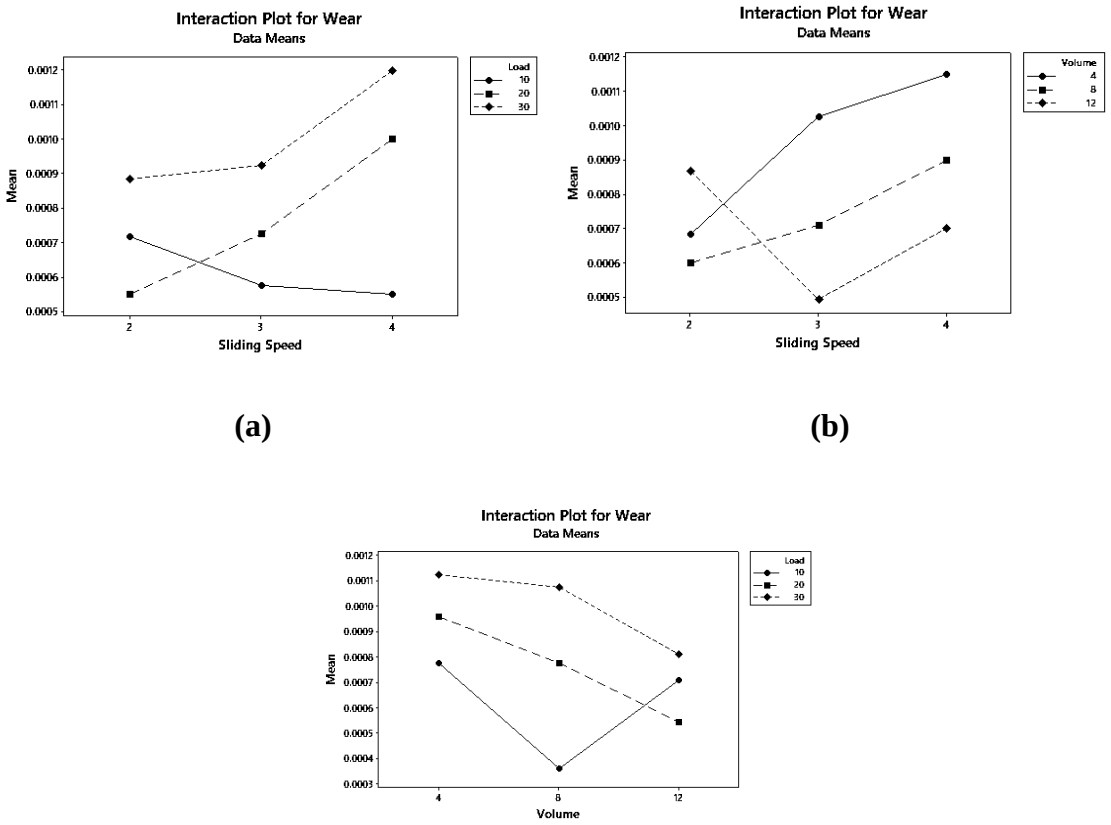

Figure 4.8 Interaction plot for S/N ratios of wear (a) S vs L, (b) S vs V, (c) V vs L

The sliding speed parameter (parameter S), applied load parameter (parameter L), and volume fraction parameter (parameter V), which also has some substantial impacts, are clearly the most significant parameters as shown by the main effects plot. Analysing an interaction plot entails identifying non-parallelism. When the lines of an interaction plot are not parallel, it indicates that there has only been nominal interaction, and when the lines cross, there have been significant interactions between the parameters. Figures 4.8 demonstrate that the parameters S and V interact strongly, but the parameters L and V and S and L interact only moderately. Therefore, it is evident from the current analysis that the sliding speed (S) is the most crucial factor affecting the friction properties of Al-RHA metal matrix composites. The process parameter sequence that produces the highest mean S/N ratio is discovered to be V1L3S1. The AL-RHA composite samples were subjected to an analysis of variance test to determine the key variables and the impact of their interactions. Each factor's % impact on AL-RHA as well as their interactions with other factors were assessed.

Table 4.9 ANOVA results of Wear

Source	DF	Adj SS	Adj MS	F-Value	P-Value	Contribution
Volume	2	0.000133	0.000066	1.54	0.355	12.80%
Load	2	0.000272	0.000136	4.64	0.187	26.21%
Sliding Speed	2	0.000063	0.000032	0.88	0.522	6.10%
Volume*Load	4	0.000123	0.000031	1.22	0.374	11.85%
Volume*Sliding Speed	4	0.000150	0.000038	1.49	0.291	14.49%
Load*Sliding Speed	4	0.000095	0.000024	0.94	0.487	9.14%
Error	8	0.000201	0.000025			19.42%
Total	26					100.00%

ANOVA is a statistical method that, when applied to the study of experimental data, might yield some significant results. This technique is particularly helpful for demonstrating the degree of significance of the influence of a factor or factors and their interactions on a certain response. It breaks out the contribution of each element and the mistake to the overall response variability. To ascertain which parameter and interaction genuinely effect the performance characteristics, an ANOVA is conducted using Minitab 17 Version. Table 4.9 provides the analysis of variance (ANOVA) findings. The F-ratio, or the ratio of the regression mean square and the mean square error, is calculated via ANOVA. The F ratio, also known as the variance ratio, is the comparison between the variance brought on by a factor's effects and the variance brought on by the error term. This ratio is used to assess how the parameters under study affect the variance of all terms included in the error term at the specified level of significance. Generally speaking, as the F value rises, so does the parameter's importance. The % contribution of each parameter is displayed in the ANOVA

table. According to the table, the most important parameter is Load (L), which contributes 26.21%. Among the parameters that affect interactions, volume fraction (V) vs. Sliding Speed(S) contributed 14.49%.

A Multiple Regression model was applied in the statistical programme "MINITAB" for confirmation. According to this model, the relationship between factors and a response variable was fitted to the observed data as a linear equation. The resulting regression equation creates an interaction between the significant factors from the ANOVA analysis, specifically Volume percent, Load, Sliding Speed, and their interactions.

The regression Equation for wear is-

Wear=0.00019444S-1.3889e-06L+1.0833e-05LS+0.00011181V-3.9583e-05VS-1.4583e-06VL-0.00012778

The S/N ratio regression equation that was created is-

S/NRatio=-2.44231S+0.00596333L+-0.104978LS+-0.948422V+0.434879VS+0.00417854VL+72.9321

Table 4.10 presents the results of the confirmation test along with a comparison to the multiple regression model under ideal circumstances. The regression model was used to generate the computed values as well as the experimental values.

Table 4.10 Confirmation test for wear and S/N ratio data

Sl No.	V	L	S	Wear	S/N Ratio	Wear(From eq)	S/N ratio(From eq)	Difference in Wear	Difference in S/N ratio
1	4	10	2	0.0004	67.9588	0.0005	65.860	0.0001	2.0988

The S/N ratio values from the experiment turn out to be 2.0988 different from those predicted by the regression equation. The experimental data and the computed S/N ratio value obtained from the regression model's equation are quite similar.

To comprehensively assess the influence of individual parameters on the wear and friction characteristics of the Al-RHA metal matrix composite, a detailed analysis is conducted. To aid in this analysis, surface plots are generated, providing valuable visual representations of the composite's behavior under different conditions. Surface plots are three-dimensional graphical representations that showcase the variations in wear and friction performance across multiple parameters. Each axis of the surface plot corresponds to a specific parameter, such as Sliding Speed (S), Load (L), or Volume Fraction (V), while the height of the surface represents the corresponding wear or friction response. By visualizing the surface plot, researchers and engineers can readily identify the trends and interactions among different parameters, helping to pinpoint the optimal operating conditions for desired wear and friction characteristics.

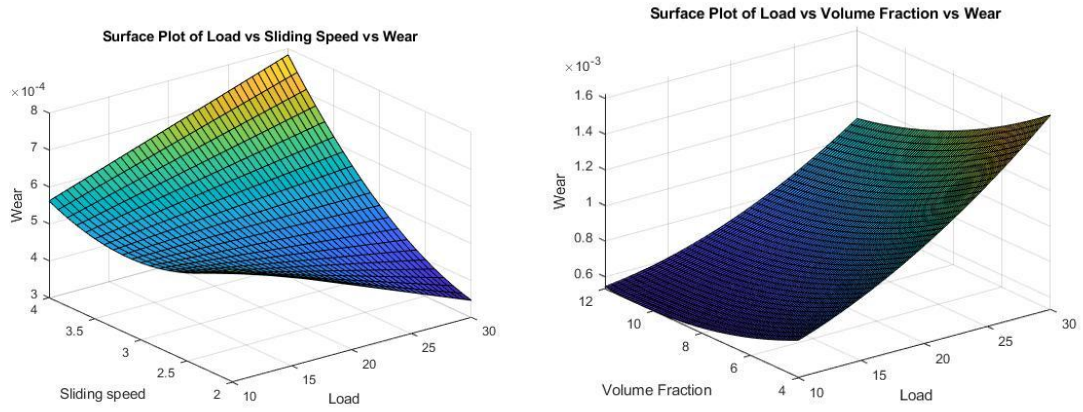

(a) **(b)**

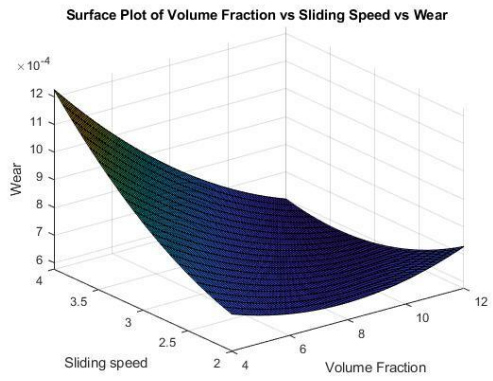

(c)

Figure 4.9 Surface plot for (a) Sliding Speed vs Load vs Wear ,(b)Volume fraction vs Load vs Wear(c)Sliding Speed vs Volume Fraction vs Wear

Figure 4.9(b),4.9(d),4.9(f) show the surface and contour plots. The graphs show that the wear value does not change monotonically as the reinforcement's volume fraction changes. Even if the efficacy is greater for the parameters of applied load and sliding speed than it is for the parameter volume fraction of reinforcement, the wear value does not change monotonically. Thus, the surface and contour plots are used to evaluate the type of wear behaviour of Al-RHA MMC. Additionally, the results from the surface plot match the ideal set of parameters, or V2L3S1, where wear is the least.

4.6 Grey Relational Analysis

It is evident from the literature study that investigations on Al-RHA composites have been conducted based on several tribological parameters, including friction, wear, and hardness. However, a combination of these tribological properties is found in industrial applications. a specific industrial application where a long service life and smooth operation are necessary. The component's design aims to simultaneously reduce wear and friction. However, it is not well understood how friction and wear interact with one another in contact. The belief that high friction causes high wear and low friction causes low wear.

Although friction and wear may have distinct backgrounds, the concept of multiple response optimisation taking both into account is worthwhile. Friction, which causes wear and heat generation in a component, is once more the primary influencing factor. Therefore, friction and wear properties must be kept to a minimum for components where less wear and low temperature are desired. Thus, minimization of friction and wear using multiple response optimisation is crucial. The friction and wear properties of Al-RHA composites are combined and analysed as one variable in the current work. By changing the testing conditions for tribological analysis, both traits are reduced. The Taguchi method is combined with grey relational analysis because this is a multiple response optimisation. Table 4.11 displays the results of the friction and wear experiments. In an earlier chapter, the method of turning friction and wear testing findings into a single grey relational grade was discussed. The lower-the-better criterion is initially used to normalise the experimental results. Table 4.12 contains the interim data that were received between each step of the procedure. Table 4.13 lists the final grey relationship grade for each experiment. Utilising the Taguchi method, the minimization of the grey relational grade is achieved using the final value of the grey relational grade as the response variable. As a performance index, grey relational grade is used in the examination of the S/N ratio. Given that the greater the grey relational grade, the

Table 4.11 Wear and CoF data from experiment

Exp No.	CoF	Wear
1	0.157	0.0004
2	0.174	0.0010
3	0.243	0.0010
4	0.202	0.0007
5	0.223	0.0010
6	0.191	0.0012
7	0.199	0.0010
8	0.266	0.0011
9	0.229	0.0013
10	0.168	0.0003
11	0.178	0.0003
12	0.174	0.0004
13	0.208	0.0006
14	0.233	0.0008
15	0.177	0.0009
16	0.175	0.0009
17	0.256	0.0010
18	0.186	0.0013
19	0.207	0.0014
20	0.145	0.0004
21	0.256	0.0003
22	0.159	0.0004
23	0.166	0.0004
24	0.253	0.0008
25	0.212	0.0008
26	0.191	0.0006
27	0.257	0.0010

Table 4.12 Normalized Friction and wear

Exp No.	Normalized Wear	Normalized Friction
1	0.884057971	0.900826
2	0.384057971	0.760331
3	0.405797101	0.190083
4	0.652173913	0.528926
5	0.369565217	0.355372
6	0.173913043	0.619835
7	0.376811594	0.553719
8	0.268115942	0
9	0.115942029	0.305785
10	0.942028986	0.809917
11	0.963768116	0.727273
12	0.855072464	0.760331
13	0.710144928	0.479339
14	0.557971014	0.272727
15	0.405797101	0.735537
16	0.47826087	0.752066
17	0.326086957	0.082645
18	0.086956522	0.661157
19	0	0.487603
20	0.847826087	1
21	1	0.082645
22	0.898550725	0.884298
23	0.876811594	0.826446
24	0.507246377	0.107438
25	0.536231884	0.446281
26	0.688405797	0.619835
27	0.362318841	0.07438

Table 4.13 Value of Δ (Deviation Sequence)

Exp. No.	Wear	Friction
1	0.115942	0.099174
2	0.615942	0.239669
3	0.594203	0.809917
4	0.347826	0.471074
5	0.630435	0.644628
6	0.826087	0.380165
7	0.623188	0.446281
8	0.731884	1
9	0.884058	0.694215
10	0.057971	0.190083
11	0.036232	0.272727
12	0.144928	0.239669
13	0.289855	0.520661
14	0.442029	0.727273
15	0.594203	0.264463
16	0.521739	0.247934
17	0.673913	0.917355
18	0.913043	0.338843
19	1	0.512397
20	0.152174	0
21	0	0.917355
22	0.101449	0.115702
23	0.123188	0.173554
24	0.492754	0.892562
25	0.463768	0.553719
26	0.311594	0.380165
27	0.637681	0.92562

Table 4.14 Grey relational coefficient (ξ)

Exp. No.	Wear	Friction
1	0.361256545	0.356932153
2	0.56557377	0.396721311
3	0.552	0.724550898
4	0.433962264	0.485943775
5	0.575	0.584541063
6	0.741935484	0.446494465
7	0.570247934	0.474509804
8	0.650943396	1
9	0.811764706	0.620512821
10	0.346733668	0.38170347
11	0.341584158	0.407407407
12	0.368983957	0.396721311
13	0.413173653	0.510548523
14	0.47260274	0.647058824
15	0.552	0.404682274
16	0.511111111	0.399339934
17	0.605263158	0.858156028
18	0.851851852	0.430604982
19	1	0.506276151
20	0.370967742	0.333333333
21	0.333333333	0.858156028
22	0.357512953	0.36119403
23	0.363157895	0.37694704
24	0.496402878	0.823129252
25	0.482517483	0.528384279
26	0.420731707	0.446494465
27	0.579831933	0.870503597

Table 4.15 Grey relational grade and its order

Exp. No.	Grey relational grade	Grey relational order
1	0.359094349	26
2	0.481147541	15
3	0.638275449	8
4	0.45995302	18
5	0.579770531	11
6	0.594214974	10
7	0.522378869	13
8	0.825471698	1
9	0.716138763	5
10	0.364218569	24
11	0.374495783	22
12	0.382852634	21
13	0.461861088	17
14	0.559830782	12
15	0.478341137	16
16	0.455225523	19
17	0.731709593	3
18	0.641228417	7
19	0.753138075	2
20	0.352150538	27
21	0.595744681	9
22	0.359353492	25
23	0.370052468	23
24	0.659766065	6
25	0.505450881	14
26	0.433613086	20
27	0.725167765	4

lower the values of friction and wear, grey relational grade must be maximised. Consequently, the larger-is-better criterion is chosen for this study. The table of the multi-response performance index (Table 4.16) provides a brief summary of the mean of the grey relational coefficient for each level of the combining parameters.

The most significant parameter affecting the tribological characterisation of the composites is parameter L, or load, according to the response table summarised in Table 4.16. According to Figure 4.10's main effects plot for the Grey relational grade, the best parameter order is one which produces the highest mean value. It is obvious that the mean value is larger for the volume fraction (V), load (L), and sliding speed (S) parameters for level 1, level 3, and level 3, respectively. Therefore, V1, L3, and S3 are in their ideal state. Al-RHA's control settings should be set to V1L3S3 (i.e., Volume fraction = 4 %, Load = 30N, and sliding speed = 4 m/s) for the least amount of wear and coefficient of friction.

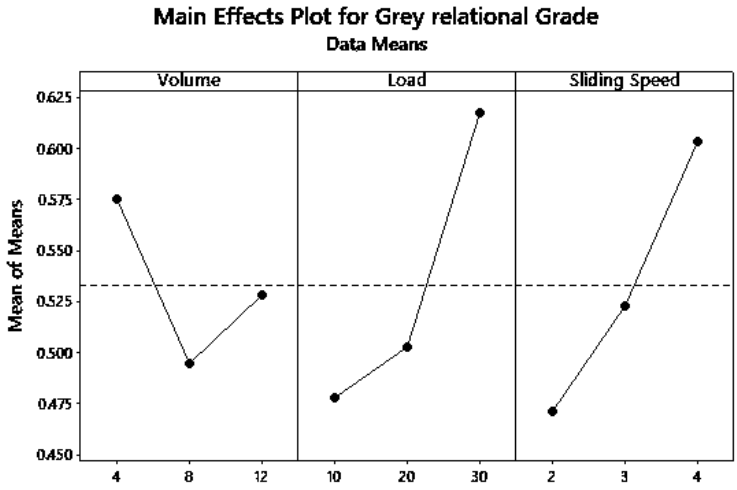

Figure 4.10 Main Effect plots for Grey Relational Grade

In Figure 4.11 the interaction graphs are displayed. The non-intersecting lines and the fact that the lines are not parallel to one another on the interaction plot between the S and L parameters indicate that there is only slight interaction between the parameters. Even in the case of S and V parameters, fewer intersecting lines are seen, but the lines are also not parallel to one another, indicating a moderate interaction between the parameters, whereas intersecting lines between L and V point to a substantial interaction between the two parameters.

Table 4.16 Response table for Grey Relational Grade

Level	Volume	Load	Speed
1	0.5752	0.4779	0.4712
2	0.4944	0.5026	0.5231
3	0.5283	0.6174	0.6035
Delta	0.0807	0.1395	0.1323
Rank	3	1	2

Total mean grey relational grade=0.53261

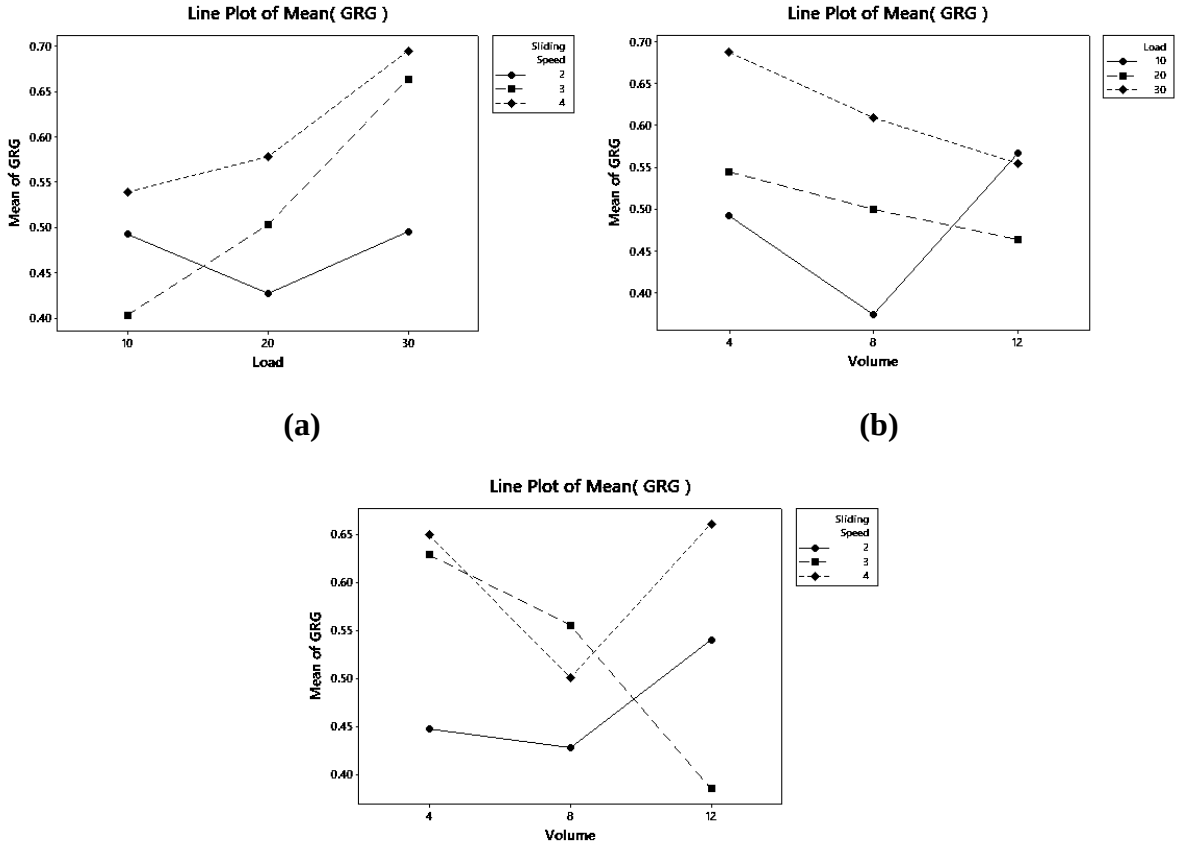

Figure 4.11 Interaction plot for Grey Relational Grade (a) Load vs Sliding Speed, (b) Volume vs Load, (c) Volume vs Sliding Speed

The ANOVA test results, as presented in Table 4.17, reveal crucial insights into the factors affecting the composite material. Among the examined parameters, the Sliding Speed

(S) emerges as the second most influential factor, contributing significantly with 15.33% to the composite's properties. However, it is worth noting that the primary contributor to the composite's behavior is the Load (L), demonstrating the highest impact with a substantial contribution of 19.10%. Moreover, the interaction between the Volume Fraction (V) and Load (L) was found to be particularly significant in influencing the composite's characteristics. This interaction effect stands out, as it contributes a notable 25.51% to the overall variations observed in the composite's properties.

Table 4.17 ANOVA results for Grey relational grade

Source	DF	Adj SS	Adj MS	F-Value	P-Value	Contribution %
Volume	2	0.02959	0.014796	1.88	0.215	5.67%
Load	2	0.09973	0.049863	6.33	0.023	19.10%
Sliding Speed	2	0.08002	0.040012	5.08	0.038	15.33%
Volume*Load	4	0.06431	0.016078	2.04	0.181	25.51%
Volume*Sliding Speed	4	0.13317	0.033293	4.22	0.040	10.00%
Load*Sliding Speed	4	0.05222	0.013054	1.66	0.252	12.08%
Error	8	0.06305	0.007881			100.00%

From the ANOVA results of Grey Relational Grade, we can see sliding speed has highest contribution to grey relational grade followed by load and volume among the interactions Volume*Load has the highest contribution followed by Load*Sliding speed.

Figures 4.12 (a), (b), and (c) depict surface plots with contour lines, illustrating the changes in Grey relational Grade as different parameter values are varied. These plots were generated using regression equations developed through Minitab software, and a MATLAB program was subsequently employed to create them. During the plot generation, one of the three parameters was kept constant at level 2, while the other two parameters were varied to

generate the surfaces. Contour lines are also present in the plots, which aid in representing a 3-dimensional (3D) surface on a 2-dimensional (2D) plane.

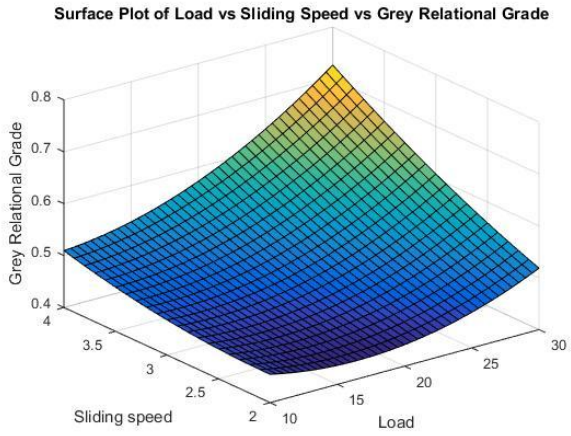

(a)

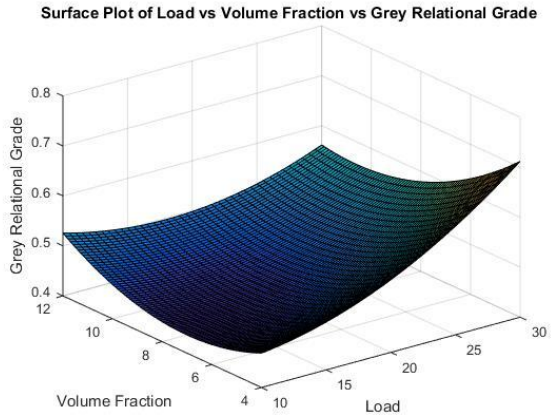

(b)

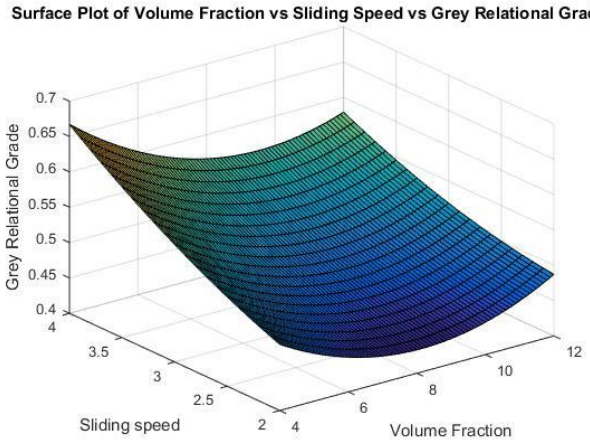

(c)

Figure 4.12 Surface plot for (a) Sliding Speed vs Load vs Grey relational Grade, (b)Volume fraction vs Load vs Grey relational Grade (c)Sliding Speed vs Volume Fraction vs Grey relational Grade

The Grey relational Grade value is determined by the combination of design factors, namely load, speed, and volume fraction of reinforcement. By analysing these surface plots, it becomes feasible to identify the region where the friction coefficient will be at its minimum. However, in the surface and contour plots of Figure 4.12, it is evident that the Grey relational Grade value does not vary monotonically with changes in the volume fraction of the reinforcement, but for sliding speed and load it varies monotonically.

The optimal combination of parameters leading to the minimum coefficient of friction is identified as V2L1S1, which corresponds to the surface plot results.

Table 4.18 Comparison of Friction and Wear

Characteristics	Optimal Combinations.
Coefficient of Friction	V2L1S1
Wear	V3L1S1
Combined COF and Wear	V1L3S3

Table 4.18 lists the ideal settings for the Al-RHA metal matrix composite's friction and wear characteristics as well as the grey relationship analysis.

4.7 Surface Morphology

From the examination of wear surface morphology, it becomes evident that the abrasive wear phenomenon is the prevailing mode of wear in the studied materials. This means that the predominant mechanism leading to the degradation of the material's surface is the result of mechanical abrasion caused by the contact with external abrasive particles or surfaces.

However, the analysis of scanning electron microscope (SEM) photos reveals that the worn surface is not solely influenced by abrasive wear. Instead, it displays a complex combination of wear mechanisms, providing a more comprehensive understanding of the material's degradation.

One of the additional wear mechanisms observed is adhesive wear. This occurs when two surfaces come into direct contact and experience bonding, leading to the transfer of material between them. Adhesive wear is often caused by the local welding and subsequent detachment of asperities (small surface irregularities) during the sliding process. This phenomenon can result in the formation of wear debris and surface irregularities.

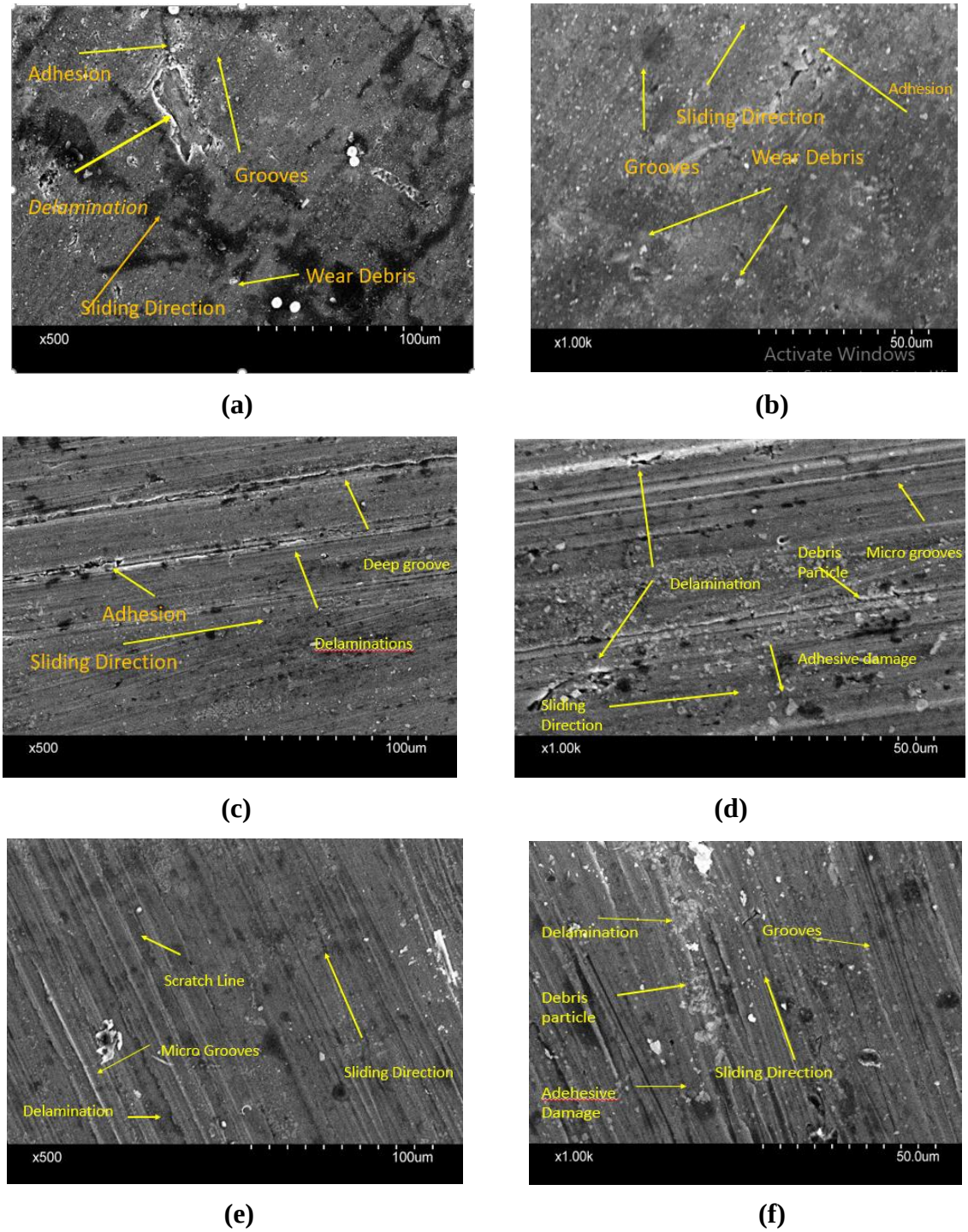

Figure 4.13 SEM image of worn-out sample
a) Al6061-4%RHA at 500X, b) Al6061-4 %RHA at 1000X,
c) Al6061-8 %RHA at 500X, d) Al6061-8 %RHA at 1000X,
e) Al6061-12 %RHA at 500X, f) Al6061-12 %RHA at 1000X

Moreover, delamination wear is another significant mechanism observed on the worn surface. Delamination wear involves the separation of material layers along the surface due to mechanical stresses and interfacial forces. This type of wear typically occurs in layered or

composite materials, and it can lead to the formation of distinctive cracks or flaking on the surface.

Thus, the SEM analysis provides valuable insights into the multiple wear mechanisms coexisting on the worn surface, indicating that abrasive wear is not the sole factor responsible for material degradation. Understanding these various wear mechanisms is crucial for developing effective strategies to mitigate wear and enhance the durability and performance of materials in real-world applications. Further investigations and analysis may help researchers and engineers design more robust and wear-resistant materials tailored to specific operational conditions.

4.8 Closure

Hardness of an Al-RHA metal matrix composite made using the stir casting method are examined in the current chapter. In the current chapter, optimisation of wear and friction for Al-RHA metal matrix composite is also explored. The Taguchi method and Grey relational grade are used during the optimisation process. According to a microstructure analysis of the wear tracks, sliding causes abrasive, adhesive, and delamination wear.

Chapter 5

Conclusion and future Scope

5.1 Conclusion

In conclusion, the conducted studies have yielded valuable findings regarding the mechanical and tribological properties of Al-RHA metal matrix composites. The hardness study revealed a notable increase in hardness value, from 70.9 VHN to 75.5 VHN, with an increase in the volume percentage (V) of rice husk from 4% to 12%. This increase can be attributed to the accumulation of strain energy at the perimeter of particles within the matrix, indicating the material's hardening behaviour.

Moving on to the friction study, the response table for the S/N ratio for COF ranked the parameters based on their delta values. The "load" (L) parameter emerged as the most influential, followed by "sliding speed" (S) and "volume fraction" (V). The ideal parameter combination for achieving the minimum coefficient of friction (COF) was identified as V2L1S1 (Volume fraction = 8%, Load = 10 N, and Sliding speed = 2 m/s), as indicated in Figure 4.4. The main effects plot in Figures 4.4 and 4.5 emphasized the significance of "load" (L) as the most crucial parameter, followed by "sliding speed" (S) and "volume fraction" (V) in determining the friction properties. Interaction plot analysis demonstrated a high interaction between "sliding speed" (S) and "load" (L) and "sliding speed" (S) and "volume fraction" (V), while the interaction between "load" (L) and "volume fraction" (V) was mild. This emphasizes the crucial role of the "load" parameter in influencing the friction properties of Al-RHA metal matrix composites.

Similarly, the wear study established the importance of the "load" (L) parameter, which ranked first in the response table, followed by "volume fraction" (V) and "sliding speed" (S). The ideal parameter combination for minimizing wear and achieving a high S/N ratio was found to be V3L1S1 (Volume fraction = 4%, Load = 30 N, and Sliding speed = 4 m/s. The main effects plot highlighted the significant impacts of "sliding speed" (S), "load" (L), and "volume fraction" (V) on wear behavior. Interaction plot analysis revealed strong interaction between "sliding speed" (S) and "volume fraction" (V), while interactions between "load" (L) and "volume fraction" (V) and "sliding speed" (S) and "load" (L) were

moderate. Thus, the study emphasized the critical role of "sliding speed" (S) in influencing the friction properties of Al-RHA metal matrix composites.

Additionally, the Grey relational analysis identified the most significant parameter affecting tribological characteristics as "load" (L), based on the response table and the main effects plot The ideal parameter order for achieving the highest mean value was found to be V1L3S3 (Volume fraction = 4%, Load = 30 N, and Sliding speed = 4 m/s), which resulted in the least amount of wear and COF. These findings highlight the importance of setting control parameters appropriately to optimize the tribological performance of the composites.

The surface plots and contour plots provided valuable visualizations of how the coefficient of friction and wear behavior are influenced by changes in the design variables. These findings helped in identifying optimal parameter combinations to achieve the desired tribological properties for Al-RHA metal matrix composites The surface plot findings aligned with the best set of parameters, V2L1S1, which exhibited the lowest coefficient of friction. Similarly, the ideal set of parameters for minimizing wear was V2L3S1.

Furthermore, the study of worn surface morphology revealed the prevalence of abrasive wear phenomena, along with the existence of adhesive, delamination, and abrasive wear mechanisms on the worn surface.

In summary, the comprehensive analyses conducted through various studies have provided valuable insights into the mechanical and tribological properties of Al-RHA metal matrix composites. Understanding the influence of the parameters and their interactions is instrumental in developing advanced composite materials with enhanced mechanical and tribological characteristics.

5.2 Future Scope

A variety of various reinforcements and their combinations of volume fraction are investigated for mechanical and tribological characterization in the current investigation. However, future researchers have a sufficient amount of still to accomplish.

- One of the key factors is the reinforcement because there are numerous additional agricultural waste reinforcements that can be combined. Additionally, the composite

can be created using different suitable metals instead of aluminium as the matrix metal.

- Rice husk ash with particle sizes ranging from 30 to 45 microns have all been investigated. This can be expanded to include various particle sizes to investigate how particle size affects the mechanical and tribological behaviour of composites.

- To create composite samples, we used the stir casting method; however, other casting methods may be applied for further research.

- For this thesis work SAE: 20W40 is used as lubricants however another types of lubricants can be tested.

- Composite samples that have undergone heat treatment to improve their properties can be further investigated, and the thesis' results can be utilised as a benchmark for composite samples that have not undergone heat treatment.

References

1. Devanathan, R., Ravikumar, J., Boopathi, S., Selvam, D.C. and Anicia, S.A., 2020. Influence in mechanical properties of stir cast aluminium (AA6061) hybrid metal matrix composite (HMMC) with silicon carbide, fly ash and coconut coir ash reinforcement. *Materials Today: Proceedings*, *22*, pp.3136-3144.

2. Rao, J.B., Rao, D.V., Murthy, I.N. and Bhargava, N.R.M.R., 2012. Mechanical properties and corrosion behaviour of fly ash particles reinforced AA 2024 composites. *Journal of composite materials*, *46*(12), pp.1393-1404.

3. Mindivan, H., Vatansever, R. and Sabri Kayali, E., 2012. Microstructure and Mechanical Properties of Dual Matrix Aluminium-Fly Ash Composites Processed via Cryomilling, Cold Compaction and Hot Extrusion. *Materials Testing*, *54*(10), pp.700-706.

4. Verma, A.S., Suri, N.M. and Kant, S., 2012. Effect of process parameter of AL-6063 based fly ash composites using Taguchi. *International Journal of Applied Engineering Research*, *7*(11), pp.1856-1859.

5. Bharathi, V., Ramachandra, M. and Srinivas, S., 2017. Influence of fly ash content in aluminium matrix composite produced by stir-squeeze casting on the scratching abrasion resistance, hardness and density levels. *Materials Today: Proceedings*, *4*(8), pp.7397-7405.

6. Dinaharan, I., Nelson, R., Vijay, S.J. and Akinlabi, E.T., 2016. Microstructure and wear characterization of aluminium matrix composites reinforced with industrial waste fly ash particulates synthesized by friction stir processing. *Materials Characterization*, *118*, pp.149-158.

7. Reddy, B.R. and Srinivas, C., 2018. Fabrication and characterization of silicon carbide and fly ash reinforced aluminium metal matrix hybrid composites. *Materials Today: Proceedings*, *5*(2), pp.8374-8381.

8. Kumar, K.R., Mohanasundaram, K.M., Arumaikkannu, G. and Subramanian, R., 2012. Effect of particle size on mechanical properties and tribological behaviour of

aluminium/fly ash composites. *Science and Engineering of Composite Materials*, *19*(3), pp.247-253.

9. Shanmughasundaram, P., Subramanian, R. and Prabhu, G.J.E.J.O.S.R., 2011. Some studies on aluminium–fly ash composites fabricated by two step stir casting method. *European journal of scientific research*, *63*(2), pp.204-218.

10. Selvam, J.D.R., Smart, D.R. and Dinaharan, I., 2013. Microstructure and some mechanical properties of fly ash particulate reinforced AA6061 aluminium alloy composites prepared by compocasting. *Materials & Design*, *49*, pp.28-34.

11. Suragimath, P.K. and Purohit, G.K., 2013. A study on mechanical properties of aluminium alloy (LM6) reinforced with SiC and fly ash. *IOSR J. Mech. Civ. Eng*, *8*(5), pp.13-18.

12. Natarajan, M.P., Rajmohan, B. and Devarajulu, S., 2012. Effect of ingredients on mechanical and tribological characteristics of different brake liner materials. *International Journal of Mechanical Engineering and Robotic research*, *1*(2), pp.2278-0149.

13. Santhosh, N., Praveena, B.A., Chandrashekar, A., Mohanavel, V., Raghavendra, S. and Basheer, D., 2022. Wear behaviour of aluminium alloy 5083/SiC/fly ash inoculants based functional composites–optimization studies. *Materials Research Express*, *9*(7), p.076513.

14. Sharma, V.K., Singh, R.C. and Chaudhary, R., 2017. Effect of flyash particles with aluminium melt on the wear of aluminium metal matrix composites. *Engineering science and technology, an international journal*, *20*(4), pp.1318-1323.

15. Kumar, P.R.S., Kumaran, S., Rao, T.S. and Natarajan, S., 2010. High temperature sliding wear behavior of press-extruded AA6061/fly ash composite. *Materials Science and Engineering: A*, *527*(6), pp.1501-1509.

16. Razzaq, A.M., Majid, D.L., Manan, N.H., Ishak, M.R. and Basheer, U.M., 2018, September. Effect of fly ash content and applied load on wear behaviour of AA6063 aluminium alloy. In *IOP Conference Series: Materials Science and Engineering* (Vol. 429, No. 1, p. 012038). IOP Publishing.

17. Rohatgi, P.K., Guo, R.Q., Huang, P. and Ray, S., 1997. Friction and abrasion resistance of cast aluminium alloy-fly ash composites. *Metallurgical and Materials Transactions A*, *28*, pp.245-250.

18. Senthilkumar, G., Manoharan, S., Balasubramanian, K. and Dhanasakkaravarthi, B., 2016. An Experimental Investigation of Metal Matrix Composites of Aluminium (Lm6), Boroncarbide and Flyash. *Australian Journal of Basic and Applied Sciences*, *10*(1), pp.137-144.

19. Shaikh, M.B.N., Arif, S. and Siddiqui, M.A., 2018. Fabrication and characterization of aluminium hybrid composites reinforced with fly ash and silicon carbide through powder metallurgy. *Materials Research Express*, *5*(4), p.046506.

20. Subramaniam, B., Natarajan, B., Kaliyaperumal, B. and Chelladurai, S.J.S., 2019. Wear behaviour of aluminium 7075—boron carbide-coconut shell fly ash reinforced hybrid metal matrix composites. *Materials research express*, *6*(10), p.1065d3.

21. Surappa, M.K., 2008. Dry sliding wear of fly ash particle reinforced A356 Al composites. *Wear*, *265*(3-4), pp.349-360.

22. Virkunwar, A.K., Ghosh, S. and Basak, R., 2019. Wear characteristics optimization of Al6061-Rice husk ash metal matrix composite using Taguchi method. *Materials Today: Proceedings*, *19*, pp.546-550.

23. Alaneme, Kenneth Kanayo, and Kazeem Oladiti Sanusi, Engineering Science and Technology, an International Journal (2015).

24. Olusesi, O.S. and Udoye, N.E., 2021. Development and characterization of AA6061 aluminium alloy/clay and rice husk ash composite. *Manufacturing Letters*, *29*, pp.34-41.

25. Prasad, D.S. and Krishna, A.R., 2012. Tribological properties of A356. 2/RHA composites. *Journal of Materials Science & Technology*, *28*(4), pp.367-372.

26. Gupta, V., Singh, B. and Mishra, R.K., 2021. Tribological characteristics of AA7075 composites reinforced with rice husk ash and carbonized eggshells. *Proceedings of*

the Institution of Mechanical Engineers, Part L: Journal of Materials: Design and Applications, *235*(11), pp.2600-2613.

27. Gladston, J.A.K., Dinaharan, I., Sheriff, N.M. and Selvam, J.D.R., 2017. Dry sliding wear behavior of AA6061 aluminium alloy composites reinforced rice husk ash particulates produced using compocasting. *Journal of Asian Ceramic Societies*, *5*(2), pp.127-135.

28. Kumar, A. and Kumar, M., 2020. Mechanical and dry sliding wear behaviour of B4C and rice husk ash reinfroced Al 7075 alloy hybrid composite for armors application by using taguchi techniques. *Materials Today: Proceedings*, *27*, pp.2617-2625.

29. B. Vinod, S. Ramanathan, M. Anandajothi, ‘‘A novel approach for utilization of agro-industrial waste materials as reinforcement with Al–7Si–0.3Mg matrix hybrid composite on tribological behavior, SN, Applied Sciences (2019) 1:62, https://doi.org/10.1007/s42452-018-0066-z.